International Journal of Pharmaceutics 667 (2024) 124895

Contents lists available at ScienceDirect

International Journal of Pharmaceutics

journal homepage: www.elsevier.com/locate/ijpharm

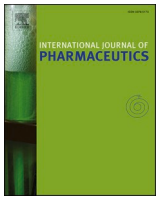

Delivery of imiquimod to intestinal lymph nodes following oral administration

Haojie Chen [a], Liuhang Ji [a], Abigail Wong [a], Yenju Chu [a,b], Wanshan Feng [a], Yufei Zhu [a], Junting Wang [a], Eleonora Comeo [a], Dong-Hyun Kim [a], Michael J. Stocks [a], Pavel Gershkovich [a,*]

[a] School of Pharmacy, University of Nottingham, Nottingham NG7 2RD, UK
[b] Department of Pharmacy Practice, Tri-Service General Hospital, Taipei 114, Taiwan

ARTICLE INFO

Keywords:
Colorectal cancer
Intestinal lymphatic targeting
Immune oncology
Toll-like receptors agonists
Imiquimod
Lymph nodes
Lipophilic prodrugs

ABSTRACT

Intestinal lymph nodes are involved in the progression of colorectal cancer (CRC). Tumours suppress the activation of dendritic cells (DCs) in draining lymph nodes, diminishing anti-cancer immune response. Imiquimod (IMQ) facilitates DCs activation *via* toll-like receptor 7, suggesting that targeted delivery of IMQ to intestinal lymph nodes can improve the treatment of CRC. This study aims to enhance the delivery of IMQ to intestinal lymph nodes by a highly lipophilic prodrug approach. Amide prodrugs were synthesised by conjugating IMQ with saturated and unsaturated medium- to long-chain fatty acids. Their potential for intestinal lymphatic transport was assessed by their affinity to chylomicrons and solubility in long-chain triglycerides. Further selection of prodrug candidates was determined by resistance to enzymatic hydrolysis in intestinal lumen and release of IMQ in the lymphatics using fasting state simulated intestinal fluid supplemented with esterases, brush border enzyme vesicles and plasma. Key pharmacokinetic parameters and biodistribution in rats were assessed for the most promising compounds, prodrugs 5 and 8. The plasma concentration–time profile of IMQ following oral administration of the prodrugs was less erratic in comparison to the administration of unmodified IMQ. The lymph-to-plasma ratios of IMQ concentration increased 1.9- and 1.7-fold using prodrugs 5 and 8 in comparison to administration of unmodified IMQ, respectively. Importantly, the average concentration of IMQ in mesenteric lymph nodes (MLN) was 11.2- and 7.6-fold higher than in plasma following the administration of prodrugs 5 and 8, respectively. Additionally, the non-specific wide distribution of IMQ into various organs and tissues was reduced with prodrugs. This work suggests that the highly lipophilic prodrug approach can efficiently deliver IMQ to intestinal lymphatics. In addition, this study demonstrates the feasibility of an amide prodrug approach for intestinal lymphatic targeting.

1. Introduction

In recent years, immunotherapies involving immune checkpoint blockade, such as programmed cell death protein 1, programmed death ligands 1 inhibitors, and adoptive cell therapy (cytotoxic T-lymphocytes antigen 4), have demonstrated promising potential in cancer treatment (Bai et al., 2021; Buchbinder and Desai, 2016; Ganesan et al., 2019; Jia et al., 2021). However, these immunotherapies were less effective in CRC than in other cancer types (Ciardiello et al., 2019; Lichtenstern et al., 2020). In the tumour microenvironment of CRC, malignant cells can develop resistance to immunotherapies by suppressing the immune response. It was reported that the response of the immune system to CRC could be hindered by the upregulated secretion of transforming growth factor beta (TGF-ß) (Ciardiello et al., 2019). In addition, the overexpression of pro-tumorigenic cytokines, such as IL-6 and IL-17, can protect the malignant colorectal epithelium by overstimulating the

Abbreviations: AUC, area under the curve; BD, biodistribution; BBMVs, Brush border enzyme vesicles; CLNs, cervical lymph nodes; CMs, Chylomicrons; CRC, colorectal cancer; DCs, dendritic cells; EDTA, ethylenediaminetetraacetic acid; FaSSIF, fasted state simulated intestinal fluid; F_{oral}, oral bioavailability; IMQ, imiquimod; IS, internal standard; IV, intravenous; ILNs, iliac lymph nodes; LNs, lymph nodes; MLNs, mesenteric lymph nodes; PO, oral administration; PK, pharmacokinetic; NaF, sodium fluoride; SD, standard deviation; TCFH, tetramethylchloroformamidinium hexafluorophosphate; TGF-ß, transforming growth factor beta; TAAs, tumour-associated antigens; Vss, volume of distribution.

* Corresponding author.
E-mail address: pavel.gershkovich@nottingham.ac.uk (P. Gershkovich).

https://doi.org/10.1016/j.ijpharm.2024.124895
Received 10 June 2024; Received in revised form 18 October 2024; Accepted 29 October 2024
Available online 31 October 2024

production of vascular endothelial growth factor and promoting cancer cell proliferation, resulting in resistance to immunotherapy (Lichtenstern et al., 2020). To overcome tumour resistance to the current immunotherapies, the combination of immunotherapeutics with different mechanisms of action was suggested (Zhu et al., 2021). The recruitment of dendritic cells (DCs) was proposed as an important strategy in cancer immunotherapy (Bai et al., 2020; Sabado, Balan, and Bhardwaj, 2017; Wculek et al., 2020). It was shown that activated DCs can present tumour-associated antigens (TAAs) to $CD8^+$ T cells and facilitate the Th1 cell differentiation of $CD4^+$ T cells (Wculek et al., 2020). In addition to stimulation of adaptive immune response, activated DCs can also enhance the innate immune response to cancer cells by stimulating natural killer cells (Zhu et al. 2021). Therefore, the simulation of DCs is an important aspect of immunotherapy of CRC.

During the progression of cancer, vascular endothelial growth factor C (a lymphangiogenic factor) is produced, activating the growth of lymphatic vessels (Stacker et al., 2014). As a result, lymphatic vessels with loose epithelial structures facilitate tumour metastasis (Kesler et al., 2013; Naxerova et al., 2017). In the metastasis of CRC, the tumour invasion pathway partially follows the mesenteric lymph nodes (MLNs) and retroperitoneal lymph nodes (such as iliac lymph nodes, ILNs), draining the lymph from the colorectal regions (Kim et al., 2004; Sasaki et al., 2023; Shu et al., 2020; Yeo et al., 2010). It was reported that in the tumour microenvironment and lymph nodes (LNs), the maturation of DCs is suppressed, and the infiltration of mature DCs is reduced, resulting in the diminished ability of the immune system to recognise cancer cells (Gulubova et al., 2012; Kusume et al., 2009).

Imiquimod (IMQ) is an agonist of toll-like receptor 7 (TLR 7). Early studies showed that IMQ facilitates the secretion of immunostimulatory cytokines, such as interferon-α (IFN- α), resulting in suppression of the tumour growth (Reiter et al., 1994; Sidky et al., 1992). It was found that the production of cytokines is regulated by the activation of DCs by IMQ binding to TLR7 through the MyD88 signalling pathway. After stimulation by IMQ, DCs transform into a mature state, promoting both innate and adaptive immune responses to the cancerous cells (Patente et al., 2019; Wculek et al., 2020). Despite the fact that in many preclinical studies TLR agonists have demonstrated great potential as anti-tumour agents, in most clinical trials TLR agonists were not very effective for cancer treatment (Frega et al., 2020; Smith et al., 2018). A previous metabolic pathway study of IMQ using human and mouse microsomes indicated that the metabolism of the drug is predominantly mediated by cytochrome P450 1A1 and 1A2 (Mescher et al., 2019). In addition, in a Phase I clinical trials of IMQ, a dose-limiting toxicity of the drug (> 50 mg) was observed in patients with refractory neoplasms (Savage et al., 1996). The systemic adverse effects, such as flu-like symptoms and nausea, and limited therapeutic success of IMQ in clinical trials could be related to its extensive non-specific distribution into tissues, and lack of targeted delivery to relevant organs, such as draining lymph nodes, enriched in DCs (Dudek et al., 2007; Wu et al., 2014; Yin et al., 2022). It was shown that naïve T cells that are located in the paracortex zone of LNs are not attracted towards activated DCs through chemotactic gradient but rather interact with them by chance. Normally, mature/activated DCs can efficiently cross-present tumour antigens to T cells at the ratio of one DC to ten T cells (Miller et al., 2004). However, in the tumour-draining lymph nodes, immature/inactivated DCs can be inhibited from the activation by two pathways. They can respond to immune suppression cytokines released from cancer cells, such as TGF-ß, or by up taking debris derived from apoptotic cancer cells, resulting in incomplete T cell activation (Dhodapkar et al., 2008; McDonnell, Robinson, and Currie, 2010). Therefore, targeted delivery of IMQ to the lymph nodes draining the colorectal region (MLNs and ILNs) could facilitate the activation of DCs and overcome the inhibitory immune responses that are regulated by cancer cells, potentially improving the treatment outcomes of people affected by CRC.

Intestinal lymphatic targeting following oral administration is one of the strategies to deliver small molecules to the MLNs. This strategy is based on the physiological pathway of dietary lipids digestion and absorption. Chylomicrons (CMs) are large lipoproteins that are assembled in the enterocytes in the presence of long-chain lipids. Due to their large size, CMs cannot penetrate blood capillaries and, therefore, are taken up selectively by lymph lacteals (Xiao, Stahel, and Lewis, 2019; Yáñez et al., 2011). Drug molecules with high affinity to CMs can be transported efficiently into the intestinal lymphatic system (Gershkovich and Hoffman, 2005). Highly lipophilic compounds with Log $D_{7.4} > 5$ and solubility in long-chain triglycerides (LCTs) > 50 mg/mL are most likely to be transported into the intestinal lymphatic system through CMs pathway (Charman and Stella, 1986; Gershkovich et al., 2008).

IMQ is not a highly lipophilic compound with a calculated log $D_{7.4}$ of 3.36 (ACD/I-lab), suggesting that this molecule is unlikely to be transported into the intestinal lymphatic system following oral administration by the CM association pathway. Previously, a lipophilic prodrug approach has been used to increase lipophilicity and hence CMs affinity of drugs, achieving intestinal lymphatic targeting (Chu et al., 2023; Kochappan et al., 2021; Lee et al., 2018; Qin et al., 2020; Quach et al., 2022). Successful lipophilic prodrugs should resist chemical and enzymatic hydrolysis in the gastrointestinal (GI) tract, but efficiently release active moieties in the intestinal lymphatic system. In addition, multiple works have suggested that the presence of LCTs in the lipid-based formulation facilitates the intestinal lymphatic transport of highly lipophilic compounds following oral administration (Porter et al., 2007). The improvement in intestinal lymphatic transport using LCT lipid-based formulation has also been observed in our previous studies (Chu et al., 2023; Feng et al., 2021a, 2021b; Gershkovich et al., 2008; Lee et al., 2018; Qin et al., 2020; Zgair et al., 2016; Zgair et al., 2017).

Therefore, the main aim of this work was to achieve targeted delivery of active IMQ to the intestinal lymph nodes draining from the colorectal region, with the ultimate goal of improvement in treatment outcomes of CRC. In most previous studies, prodrug candidates for intestinal lymphatic targeting following oral administration were based on the ester bond structure (Chu et al., 2023; Kochappan et al., 2021; Lee et al., 2018; Qin et al., 2020; Quach et al., 2022). However, Han *et al.* reported a lipophilic prodrug of mycophenolic acid that was conjugated with an alkyl chain *via* an amide bond. The approach was found to be not efficient for targeting intestinal lymphatics following oral administration since the amide prodrug did not release the active moiety efficiently within the lymphatic system (Han et al., 2014). IMQ only has a primary amine as a prodrug-able functional group that can be conjugated with lipophilic groups through an amide bond. However, IMQ release from the amide prodrugs could be efficient due to the electron resonance between the amine and imidazoquinoline in IMQ.

2. Materials and methods

2.1. Materials

Imiquimod (IMQ, CAS: 99011-02-6) was purchased from Key Organics Ltd. (Cornwall, UK). Porcine liver esterase, Bradford assay kit, olive oil, porcine liver esterase and Intralipid® were bought from Sigma-Aldrich Inc. (Gillingham, UK). The alkaline phosphatase and leucine aminopeptidase activity assay kits were purchased from Abcam (Cambridge, UK). Rat plasma was purchased from BIOIVT (Burgess Hill, UK). Propylene glycol (European Pharmacopeia level) and ammonium formate were purchased from Fisher Scientific (Leicestershire, UK). Other agents and solvents were purchased from commercially available sources and were HPLC or LC-MS grade.

2.2. Design of IMQ lipophilic prodrugs

IMQ lipophilic prodrugs were designed based on a previously reported *in silico* model for the prediction of affinity to CMs (Gershkovich et al., 2008). IMQ was conjugated to saturated and unsaturated fatty acids with different chain lengths. The physicochemical properties of

IMQ and its prodrugs were calculated using ACD/I-Labs and then imported into the *in silico* model to predict the CM association percentage of compounds (Gershkovich et al., 2008). Prodrugs with high predicted affinity to CM were synthesised as described below.

2.3. General chemical reaction for IMQ amide prodrugs

The amidation of imiquimod was introduced with coupling reagents *N, N, N′, N′*-tetramethylchloroformamidinium hexafluorophosphate (TCFH) and *N*-methylimidazole (NMI) as previously reported (Beutner et al., 2018). Briefly, the corresponding fatty acids (0.3 mmol) were activated with TCFH (0.35 mmol) and NMI (1.05 mmol) in 2 mL anhydrous *N*-methyl-2-pyrrolidone (NMP) and stirred under nitrogen at 45°C for 30 min. Then, IMQ (0.39 mmol) was added to start the amidation and the mixture was stirred for 24 h. The reaction process was monitored by thin-layer chromatography (TLC) and LC-MS/MS. The crude product was purified by flash chromatography using a 12 g silica gel-packed column and hexane–ethyl acetate (50:50, v/v) as the mobile phase. The schematic presentation of chemical synthesis and all IMQ prodrug structures are shown in Fig. 1. Characterisation of all synthesised prodrugs is described in **Characterization of purified prodrugs** (**Supplementary material**).

2.4. In vitro estimation of CM association

The associations of compounds with artificial CM-like emulsion were assessed by means of previously reported methodology (Chu et al., 2023; Gershkovich et al., 2008; Gershkovich and Hoffman, 2005; Lee et al., 2018; Qin et al., 2020). Briefly, the CM-like emulsion was obtained by dilution of Intralipid® with Dulbecco's phosphate-buffered saline to obtain the concentration of triglycerides of 1 mg/mL. For the association experiment, tested compounds were incubated with artificial CMs at 37 °C at a final concentration of 1.75 μM with magnetic stirring at 170 rpm for one hour. This mixture was then transferred into polyallomer ultracentrifuge tubes and layered with KBr gradient solution with different densities as previously reported (Gershkovich and Hoffman, 2005). After ultracentrifugation (SORVALL Ultracentrifuge, TH-641 Rotor) at 268,350 *g* at 15 °C for 35 min, the top layer of white artificial CMs was collected and analysed using HPLC-UV to determine the amount of tested compounds that associated with emulsion particles.

2.5. Long-chain triglyceride solubility

The solubility of tested compounds in long-chain triglycerides was assessed using olive oil (Chu et al., 2021; Chu et al., 2023). Five to six milligrams of the tested compound were added to 100 μL of olive oil at 37 °C and stirred for 72 h. At the end of the study, if the added compound was dissolved entirely, no additional amount of the compound would be added. After incubation, the remaining drug particles were removed using Costar Spin-X Centrifuge tubes with a 0.22 μm filter *via* centrifugation at 2,400 *g* for 10 min at 37 °C. The filtrates were 10-fold diluted with acetone, following by 100-fold dilution with ethanol. Some samples underwent additional 10-fold dilution with MeOH, depending on the expected concentration range of tested compounds in triglycerides. The concentrations were determined by means of HPLC-UV. All experiments were performed in triplicate.

2.6. In vitro and ex vivo assessments of biotransformation of prodrugs to IMQ

2.6.1. Preparation of biorelevant media

Brush border enzyme vesicles (BBMVs) were collected from rat small intestine using a previously reported protocol (Kessler et al., 1978). Briefly, fresh jejunum and ileum were harvested from SD male rats (weight 270 – 350 g) and flushed with ice-cold saline to remove the intestinal contents. BBMVs were extracted using 12 mM Tris/chloride buffer (pH = 7.1) containing 300 mM mannitol. BBMVs pellets were purified using centrifugation at 27000 x g for 30 min at 4 °C. Alkaline phosphatase and leucine aminopeptidase were selected as representative activity control enzymes in BBMVs, and their activities were measured using commercial kits (Abcam, Cambridge, UK). The total protein concentration of BBMVs was measured using Bradford reagent with bovine albumin as a reference standard. The BBMVs experimental medium was completed by adjusting protein concentration to 1 mg/mL with 10 mM Tri/HEPES (pH = 7.1, containing 50 mM mannitol).

The fasted state simulated intestinal fluid (FaSSIF) was prepared using a previously reported protocol (Marques, 2004). On the day of the experiments, the FaSSIF + esterase incubation medium was completed by adding porcine hepatic esterase to the FaSSIF at a concentration of 20 IU/mL (Chu et al., 2023; Lee et al., 2018; Qin et al., 2020).

2.6.2. Biotransformation experiment

The biotransformation of the prodrugs to IMQ was assessed in rat plasma, FaSSIF supplemented with 20 IU/mL esterase, and BBMVs

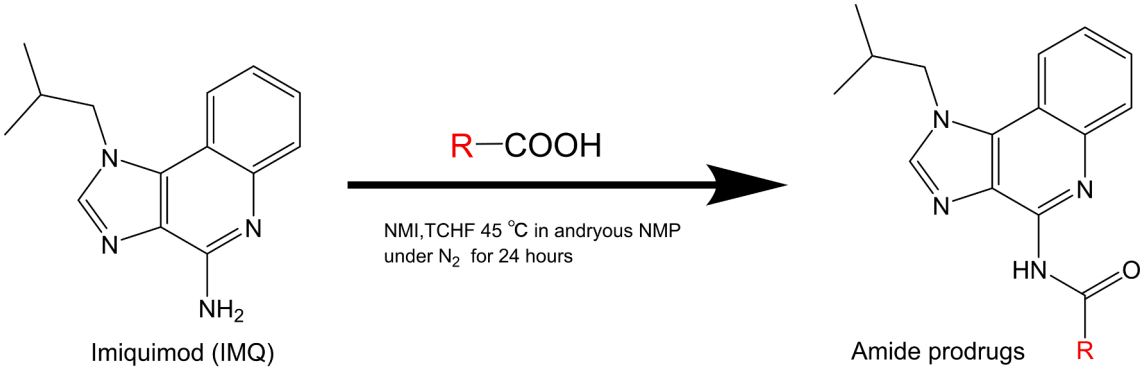

Saturated fatty acid	Unsaturated fatty acid
1:R = $CH_3(CH_2)_8$	5:R = $CH_3(CH_2)_3CH{=}CH(CH_2)_7$
2:R = $CH_3(CH_2)_{12}$	6:R = $CH_3(CH_2)_5CH{=}CH(CH_2)_7$
3:R = $CH_3(CH_2)_{14}$	7:R = $CH_3(CH_2)_7CH{=}CH(CH_2)_7$
4:R = $CH_3(CH_2)_{16}$	8:R = $CH_3(CH_2)_4CH{=}CHCH_2CH{=}CH(CH_2)_7$

Fig. 1. Chemical synthesis conditions and structures of lipophilic prodrugs of IMQ.

media as reported in previously published protocols (Chu et al., 2023; Lee et al., 2018; Qin et al., 2020). Stock solutions of prodrugs were prepared in DMSO at a concentration of 1 mM. The biorelevant media were pre-heated at 37 °C for 10 min. The assay was initiated by spiking prodrug stock solution into the biorelevant media to reach a final concentration of 10 μM for rat plasma and FaSSIF with esterase, or 2 μM for BBMVs. The final concentration of the prodrugs in the experimental media was lower than the Michaelis-Menten constant (K_m = 4.696 μM, **Figure S1**, **Supplementary material**). The incubation was performed in a thermo-controlled orbital incubator (Thermo Scientific MaxQ4000, Waltham, MA, USA) at 37 °C and 200 rpm. One hundred and twenty microliters of incubated mixtures were collected at pre-determined time points, and 360 μL of ice-cold acetonitrile was added to terminate the reaction. The concentrations of IMQ and its prodrugs in samples were determined using a validated HPLC-UV methodology, as described below. All experiments were performed in triplicates.

2.7. Formulations of IMQ and its prodrugs

The oral lipid-free formulation of IMQ was prepared by dissolving IMQ powder in 0.05 N HCl at a concentration of 8 mg/mL. After IMQ powder was fully dissolved, the pH of the solution was measured and confirmed to be in the range of 2 – 2.5. The IV bolus formulation of IMQ was prepared by a 10-fold dilution from the oral lipid-free formulation with 80:20 propylene glycol/water (v/v) to a final IMQ concentration of 0.8 mg/mL. The pH of the IMQ IV formulation was adjusted to 6.5 using a 4 N NaOH solution.

Prodrugs 5 and 8 were administered to animals at an equimolar dose of IMQ. The oral formulations of prodrugs 5 and 8 were prepared by dissolving prodrugs in olive oil at a concentration of 14.9 mg/mL and 16.9 mg/mL, respectively. The IV bolus formulations of prodrugs 5 and 8 were prepared by dissolving prodrugs in 80:10:10 propylene glycol/water/ethanol (v/v/v) at a concentration of 1.49 mg/mL and 1.69 mg/mL, respectively.

2.8. Animal studies

2.8.1. Animals

The protocols for pharmacokinetic (PK) and biodistribution (BD) studies for IMQ and its prodrugs were reviewed and approved by the University of Nottingham Ethical Committee under the Animals [Scientific Procedures] Act 1986. Male Sprague Dawley (SD) rats (275–300 g body weight) were purchased from Charles River Laboratories (UK) and housed in the Bio Support Unit at the University of Nottingham in an environmentally controlled room (12 h light/dark cycle) with free access to food and water for at least seven days. The weight of rats before the PK or BD study was 300–350 g.

2.8.2. Pharmacokinetic study

The right jugular vein cannulation surgery was performed under general isoflurane gas-induced anaesthesia. After the surgery, animals were allowed to recover for two nights with free access to food and water. Animals were fasted for 10 h prior to the drug administration with free access to water. Food was provided to animals 5–6 h after the drug administration.

In the IMQ pharmacokinetic study, rats were divided into oral lipid-free, oral lipid-based and IV bolus groups. For the IMQ oral lipid-free group, 8 mg/kg of IMQ in the lipid-free formulation (8 mg/mL) was administered by oral gavage. This dose was confirmed as safe in previous studies (Kang et al., 2019; Soria et al., 2000). For the IMQ oral lipid-based group, the lipid-free formulation was administered by oral gavage at the same dose, followed by the same volume of olive oil as the lipid-free formulation. After the formulation administration, 1 mL of water was administered by oral gavage to facilitate the emulsification of the administered oil. Following the administration, blood samples were collected from the cannula at pre-determined time points: 0.5, 1, 2, 4, 8, 12, 16, 20, 24 and 28 h. For the IMQ IV group, IMQ IV formulation at the dose of 0.8 mg/kg was administered *via* the jugular vein cannula as an IV bolus over 30 s. Whole blood was sampled at pre-determined time points: 5, 15, 30, 60, 90, 120, 180, 240 and 300 min. All samples were collected into 1.5 mL Eppendorf tubes containing EDTA as an anticoagulant.

In the pharmacokinetic study of IMQ lipophilic prodrugs, prodrug formulations were freshly prepared on the day of the experiment and administered *via* oral gavage (at the doses of 14.9 mg/kg for prodrug 5 and 16.9 mg/kg for prodrug 8) or IV bolus (at the doses of 1.49 mg/kg for prodrug 5 and 1.69 mg/kg for prodrug 8). Blood was sampled at pre-determined time points: 0.5, 1, 1.5, 2, 3, 4, 5, 6, 8 and 12 h following oral administration and 5, 15, 30, 60, 90, 120, 180, 240, 300 and 360 min following IV administration. Blood samples were collected into 1.5 mL Eppendorf tubes containing EDTA, as well as sodium fluoride (NaF, final concentration at 10 mg/mL) to prevent the release of IMQ following the collection of the samples. Plasma was obtained by centrifugation (1,160 *g* for 10 min at 10 °C) and stored at −80 °C until analysis.

2.8.3. Biodistribution study of IMQ and its prodrugs

In the BD study of IMQ, the drug was administered by oral gavage to rats in the lipid-free formulation followed by oral gavages of olive oil and water, as described in **section 2.8.2**. In the BD study of prodrugs, the compounds were administered to animals by an oral gavage in the lipid-based formulation followed by 1 mL of water. At predetermined time points (1.5, 2, 6, and 28 h for IMQ; 1.5 and 6 h for prodrugs), blood samples were collected from the vena cava under terminal anaesthesia. After animals were sacrificed by cervical dislocation, the mesenteric lymph fluid sample was immediately collected from the superior mesenteric lymph duct using a syringe connected to a 23G needle. Other tissues, including MLNs, ILNs, deep and superficial cervical lymph nodes (CLNs), brain, spleen, kidney, liver, skeleton muscle (right thigh) and intestinal contents, were then also harvested from the cadavers.

Plasma and serum were separated by centrifugation of non-coagulated and coagulated whole blood at 1,160 *g* for 10 min at 10 °C, respectively. All harvested tissues were weighed. Large organs, including kidney, brain, liver, skeleton muscle (right thigh) and spleen, were homogenised in 10 mg/mL NaF solution at a ratio of 1:3 (w/v) using a Polytron® PT 10–35 GT homogeniser (Kinematica, Malters, Switzerland). Intestinal contents, including liquid and solids, collected from small intestines, large intestines and recta were homogenised in NaF solution (10 mg/mL) at a ratio of 1:10 or 1:20, depending on the expected concentration of tested compounds in tissues. Lymph nodes were placed in 1.5 mL Eppendorf tubes with 3–5 Stainless Steel Beads (Next ADVANCE, Web Scientific, USA) and NaF solution (10 mg/mL) was added to obtain at least 100 μL volume of samples. Lymph nodes were then homogenised using a Bullet Blender 24 Gold (Next Advance, USA).

All processed samples were kept at −80 °C until analysis. Concentrations of IMQ, prodrug 5 and prodrug 8 in the processed *in vivo* samples were determined using LC-MS/MS methodology as described in **Section 2.9**.

2.9. Bioanalytical methodology

2.9.1. Sample preparation

Two instruments were used to determine the concentration of analytes in this work. Samples collected from *in vitro* and *ex vivo* experiments had high expected concentrations (**sections 2.4, 2.5 and 2.6**) and were analysed using HPLC-UV. Samples collected from *in vivo* studies (**Section 2.8**) were analysed using LC-MS/MS.

All analysed samples underwent the same preparation procedure but with different sample volumes. Three-hundred and sixty microliters of cold acetonitrile (−20 °C) were added to 120 μL of samples generated in *in vitro* experiments (or 100 μL for *in vivo* samples) for protein precipitation, followed by the addition of 12 μL of 50,000 ng/mL propranolol

solution in MeOH (or 10 µL of 5,000 ng/mL propranolol for *in vivo* samples) as an internal standard (IS). Liquid-liquid extraction was performed by vortex-mixing samples with 3 mL of MTEB for 10 min. After centrifugation at 1160 *g* at 10 °C for 10 min, the upper organic layer was transferred to clean glass test tubes and evaporated to dryness at 40 °C under nitrogen flow. Samples were reconstituted with 100 µL of 65:35 water/methanol (v/v) (60 µL for *in vivo* samples) and transferred into HPLC vials. The validation of the bioanalytical methods is shown in **Validation of bioanalytical methods (Supplementary material)**.

2.9.2. HPLC-UV

The HPLC system consisted of a Waters Alliance 2695 separations module equipped with a Waters 996 photodiode array detector. Chromatographies were monitored at 319 nm for all analytes. A C18 150 x 2 mm, 5 µm particle size reverse phase column (Gemini-LC-column, Phenomenex, US) connected to a 3 µm particle size guard column was used to achieve separation. The column temperature was maintained at 40 °C and autosampler at 4 °C. The samples were injected into the HPLC system at a volume of 60 µL. Chromatograms were processed and analysed using Empower™ 2 software. The detailed HPLC chromatography conditions and retention times for all tested compounds are shown in **Table S1 (Supplementary material)**.

2.9.3. LC-MS/MS

The LC-MS/MS system consisting of an AB Sciex API Qtrap4000 tandem mass spectrometry detector coupled with a SHIMADZU LC-10AD binary pump and a SHIMADZU SIL-HTc autosampler was used for analysis. The conditions of the mobile and solid phases were the same for the HPLC-UV (**section 2.9.2**). The injection volume for the LC-MS/MS method was 10 µL. The ionisation of analytes was conducted in positive mode with multiple reaction monitoring. The remaining MS conditions were set as follows: ion spray voltage 5,000 V; temperature 350 °C; curtain gas 30 psi; ion source gas 1 and gas 2 40 psi; entrance potential 10 V. Other parameters and monitored ion pairs in Q1 and Q3 are shown in **Table S2 (Supplementary Material)**.

2.10. Pharmacokinetic calculations and statistical analysis

Pharmacokinetic parameters were calculated from the plasma concentration profiles by non-compartmental analysis approach using Phoenix® WinNonlin®6.3 software (Pharsight, Mountain View, CA, USA). The method of calculation Linear up Log down was applied to compute the area under the curve (AUC). Statistical analysis was performed on GraphPad Prism version 10 (GraphPad Software, Inc., San Diego, CA, USA). All data are shown as mean ± deviation (SD). One-way analysis of variance (ANOVA) followed by Dunnett's or Turkey's multiple comparisons, or unpaired *t*-test were used where appropriate. A significant difference was stated when a *p*-value was below 0.05.

3. Results

3.1. Affinity of IMQ and its prodrugs to CM

The affinity to CMs is a key parameter for the prediction of the intestinal lymphatic transport of drugs following oral administration in the presence of long-chain triglycerides or fatty acids (Gershkovich and Hoffman, 2005). Compounds 1–4 are highly lipophilic prodrugs of IMQ conjugated with saturated fatty acids, including decanoic, myristic, palmitic, and stearic acids, respectively. As shown in Table 1, IMQ has negligible predicted affinity to CM, while all designed prodrugs have moderate (>50 %) to high (> 90 %) predicted affinity. With an extension of chain length from 10 to 14 carbons, the predicted CMs association increases from moderate to high. Therefore, prodrugs 1–4 were synthesised, and their experimental association with artificial CM-like emulsion was assessed. As predicted, IMQ had indeed no affinity to artificial CM, while the affinities of prodrugs 1–4 were substantial (Table 1). Due to a prolonged release rate of IMQ from prodrugs 1–4 observed in plasma (**Section 3.3**), the second generation of prodrugs with unsaturated fatty acids (prodrugs 5–8) was designed and synthesized, including myristoleic, palmitoleic, oleic and linoleic acids conjugates. These unsaturated fatty acids are of the same chain length as saturated fatty acids used in prodrugs 1–4. No difference was found in the affinity to CMs between the saturated and unsaturated prodrugs (Table 1).

3.2. Long-chain triglycerides solubility

The solubilities of prodrugs in olive oil are summarised in Table 1. IMQ, and prodrugs 1 and 2 were in powder form. Following a 72-hour solubility test, undissolved particles of IMQ and prodrugs 1 and 2 were still visually noticeable in the oil phase. Prodrugs 3 and 4 were in a wax form, while prodrugs 5–8 were in an oil form. By the end of the solubility test, prodrugs 3–8 were fully dissolved in olive oil, suggesting triglyceride solubility above 50 mg/mL for these compounds.

3.3. Biotransformation of prodrugs to IMQ in biorelevant media

The biotransformation of prodrugs to IMQ was estimated using two biorelevant media representing the intestinal tract: FaSSIF with added esterase activity and BBMVs, as well as rat plasma as a surrogate of

Table 1
Calculated physicochemical properties, predicted and experimental CMs associations, and triglycerides solubilities of IMQ and its prodrugs.

	Compounds								
	IMQ	1	2	3	4	5	6	7	8
Log D 7.4 [a]	3.46	6.35	8.31	9.2	10.09	7.95	8.84	9.72	9.36
Log P [a]	3.46	7.12	9.24	10.31	11.37	8.73	9.79	10.85	10.33
Log P – Log D [a]	0	0.77	0.93	1.11	1.28	0.78	0.95	1.13	0.97
PSA [a]	86.11	59.81	59.81	59.81	59.81	59.81	59.81	59.81	59.81
H-Acceptors [a]	7	3	3	3	3	3	3	3	3
FRB [a]	19	12	16	18	20	15	17	19	18
Density [a]	1.28	1.11	1.08	1.06	1.05	1.07	1.06	1.04	1.04
Molar Volume [a]	187.7	352.7	416.9	449	481.1	416.9	449	481.1	481.1
H-Donors [a]	1	1	1	1	1	1	1	1	1
Predicted association (%)	1.8	50.1	93.8	98.1	99.4	91.2	97.3	99.2	98.9
Assessed association (%)[b] (n = 3)	< 1.75	73.8 ± 4.1****	78.4 ± 11.9****	76.4 ± 6.0****	66.7 ± 11.4****	70.3 ± 14.5****	64.4 ± 28.8****	76.8 ± 13.5****	76.5 ± 19.1****
Triglyceride solubility (µg/mL) (n = 3)	7.4 ± 1.0	2510 ± 210	46400 ± 7300	> 5000	> 5000	> 5000	> 5000	> 5000	> 5000

One-way ANOVA, followed by Dunnett's comparison, was used for statistical analysis. Asterisks denote significance against IMQ.****,$p < 0.0001$.

[a] Calculated by ACD/I-Lab.

[b] Affinity of compounds to artificial CMs (prepared with Intralipid®).

lymph (Fig. 2 **A-C**) (Chu et al., 2023; Lee et al., 2018; Qin et al., 2020). The rate of conversion was expressed as the half-lives of prodrugs and summarised in Fig. 2 **D**. It should be noted that the esterase used in the FaSSIF + esterase assay is, in fact, a crude extract from porcine liver only characterised for esterase activity, but also contains additional enzymes with unquantified activity. It was found that IMQ was released from the amide prodrugs quite efficiently in the presence of this liver extract in the FaSSIF (Fig. 2 **A and D**). BBMVs medium was also used to estimate the biotransformation of IMQ amide prodrugs. All tested prodrugs were stable in the presence of BBMVs (Fig. 2 **B and D**). Additionally, in this assay, rat plasma was used as a surrogate for lymph fluid as previously described, since they share similar enzymatic composition (Fanous et al., 2007). Only prodrugs 1, 5, 6 and 8 efficiently released > 50 % of IMQ by the end of 2 h incubation in rat plasma (Fig. 2 **C and D**). Moreover, as shown in **Figure S7** (**Supplementary material**), an increase in the fatty acid carbon chain from 10 to 18 (prodrugs 1–4) resulted in prolonged half-lives in FaSSIF + esterase medium and rat plasma. In addition, comparing the half-lives of prodrugs 2 vs 5, 3 vs 6, and 4 vs 7 or 8 in these two media, it was found that unsaturation resulted in the reduction of the half-lives.

Taking together the artificial CMs affinity, long-chain triglycerides solubility and the rate of IMQ release in the biorelevant media, prodrugs 5 and 8 were selected as the most promising candidates to proceed to *in vivo* studies.

3.4. Pharmacokinetics of IMQ, prodrugs 5 and 8

The pharmacokinetic (PK) profiles of IMQ in plasma were generated following intravenous (IV) bolus and oral (PO) administration (without and with lipids) in rats (Fig. 3). Pharmacokinetic parameters of IMQ derived from plasma concentration–time profiles are summarised in Table 2 and **Table S3** (**Supplementary material**). Following IV bolus administration of IMQ, a relatively short half-life of IMQ (0.73 ± 0.05 h) was found. Interestingly, although the lipophilicity of IMQ is moderate (Log P = 3.46), the apparent volume of distribution (V_{ss}) of IMQ after IV administration was quite high (3376.3 ± 1842.0 mL/Kg). The plasma concentration–time profiles of IMQ following oral administration suggest that the oral absorption of IMQ is prolonged and erratic with no obvious T_{max} (Fig. 3 **B**). Moreover, the oral absorption of IMQ varied significantly between rats, resulting in substantial variability of IMQ concentrations in plasma. In some rats, IMQ concentrations were undetectable after 20 h, while in others, the plasma concentration of IMQ remained high for a prolonged period. The oral bioavailability (F_{oral}) of IMQ was below 10 %, and there was no statistically significant difference in F_{oral} between the IMQ lipid-free and IMQ lipid-based administrations.

The plasma concentration–time profiles of IMQ released from prodrugs 5 and 8 were generated following IV and PO administration of prodrugs (Fig. 4). A statistically significant difference was found between the terminal slope half-lives ($t_{1/2}$) of IMQ following IV

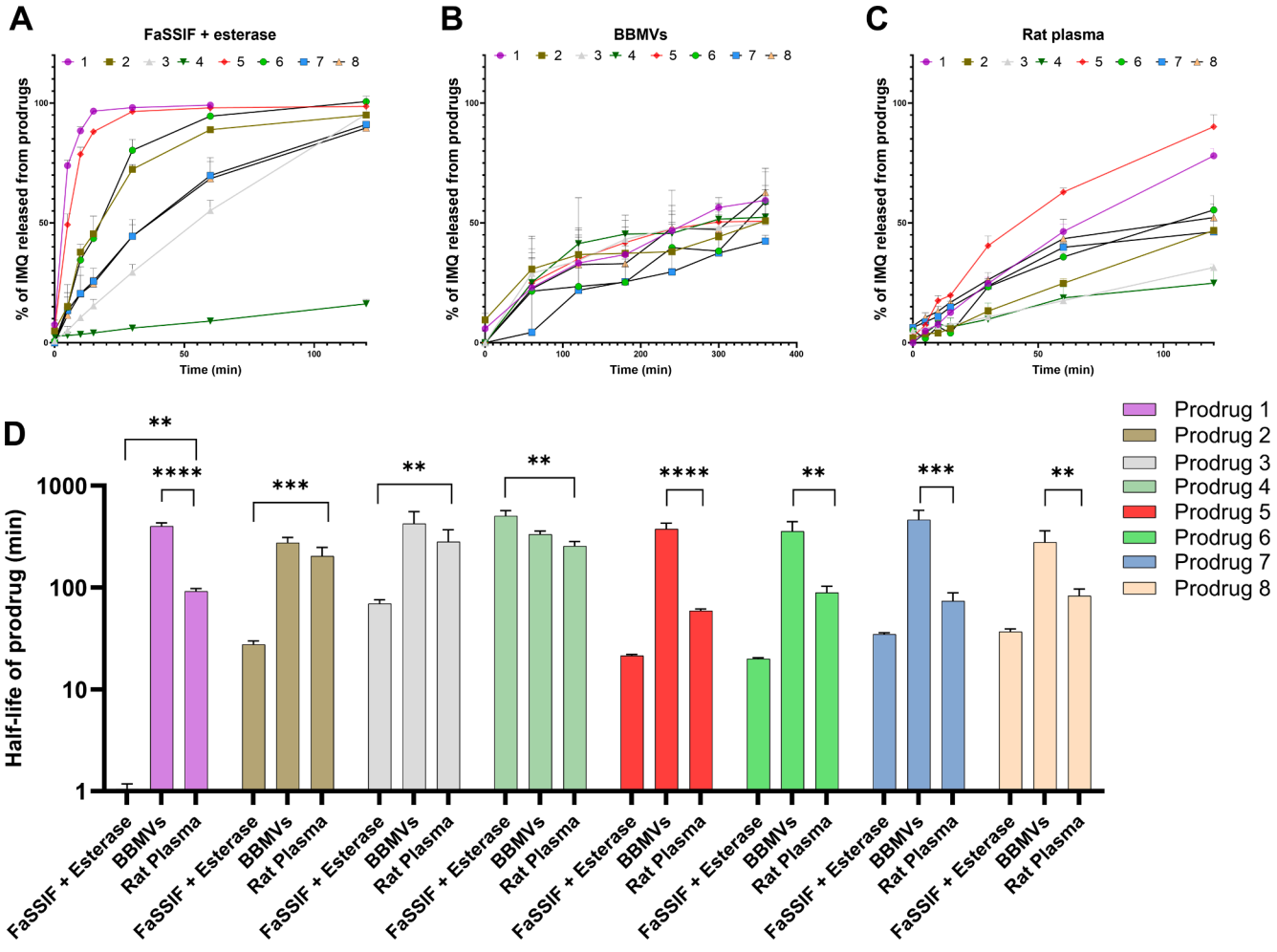

Fig. 2. The biotransformation of prodrugs to IMQ (n = 3, mean ± SD). Panels (A), (B) and (C) show the kinetics of IMQ release from prodrugs in FaSSIF with porcine esterase (20 IU/mL), BBMVs (1 mg/mL of total protein level) and rat plasma, respectively. Panel D shows the half-lives ($t_{1/2}$) of prodrugs in tested relevant media. One-way ANOVA, followed by Dunnett's comparison, was used for statistical analysis. Asterisks denote significance against the half-life of the prodrug in plasma. **, $p < 0.01$; ***,$p < 0.001$; ****,$p < 0.0001$.

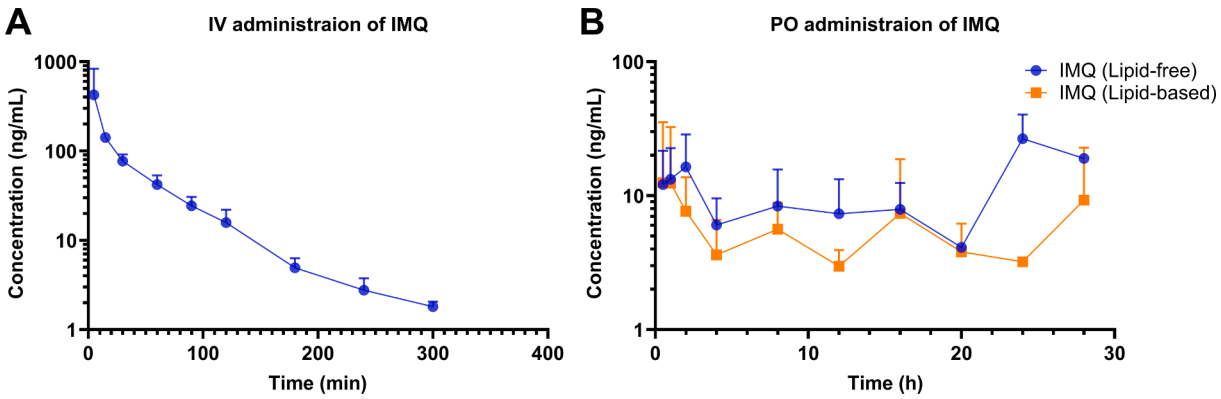

Fig. 3. Plasma concentration–time profile in rats following administration of IMQ (mean ± SD). Panel (A) shows the profile following an IV bolus of IMQ (0.8 mg/Kg, n = 4); Panel (B) shows the profile following oral administration of IMQ (8 mg/Kg) in lipid-free formulation (n = 6) and with lipids (n = 5).

Table 2
Pharmacokinetic parameters of IMQ following administrations of different compounds to rats: 1) IMQ (0.8 mg/kg for IV and 8 mg/kg for PO); 2), prodrug 5 (1.49 mg/kg for IV and 14.9 mg/kg for PO); and 3) prodrug 8 (1.69 mg/kg for IV and 16.9 mg/kg for PO) (mean ± SD).

Compound dose	Imiquimod			Prodrug 5		Prodrug 8	
Route of administration	IV (n = 4)	PO (lipid-free) (n = 6)	PO (lipid-based) (n = 5)	IV (n = 4)	PO (n = 6)	IV (n = 4)	PO (n = 5)
AUC_{inf} (h·ng/mL)	203.2 ± 95.4	–	–	105.6 ± 26.5	415.4 ± 225.1	97.3 ± 27.6	531.6 ± 398.3
AUC_{last} (h·ng/mL)	200.7 ± 96.0	168.3 ± 90.0	136.3 ± 85.3	102.5 ± 26.1	313.8 ± 198.1	95.4 ± 27.4	404.3 ± 301.3
C_0 or C_{max} (ng/mL)	274.9 ± 60.9	26.7 ± 14.6	17.1 ± 10.9	390.2 ± 243.8	78.0 ± 66.3	310.4 ± 274.7	72.8 ± 37.7
CL (mL/h/kg)	4468.5 ± 1569.8	–	–	–	–	–	–
V_{ss} (mL/kg)	3376.3 ± 1842.0	–	–	–	–	–	–
$t_{1/2}$ (h)	0.73 ± 0.05[b]	–	–	1.5 ± 0.2[b] *	2.2 ± 0.9	1.1 ± 0.2[b] *	4.9 ± 2.7
T_{max} (h)	–	0.5 - 28	2 - 28	–	2 - 6	–	2—6
F_{oral} (%) [a]	–	8.3 ± 4.5[b ns]	6.7 ± 4.2[b ns]	–	15.6 ± 9.8[b ns]	–	20.1 ± 15.0[b ns]

AUC_{inf} area under the curve from time zero to infinity; AUC_{last} area under the curve from time zero to the last observed time point (0 – 300 min for IV administration of IMQ; 0 – 28 h for PO administration of IMQ; 0 – 360 min for IV administration of prodrugs; 0 – 12 h for PO administration of prodrugs); C_{max}, maximum observed concentration; C_0, concentration extrapolated to time zero; CL, clearance; V_{ss}, volume of distribution at steady state; $t_{1/2}$, half-life; F_{oral}, absolute oral bioavailability. All values are presented as mean ± SD.

[a] the absolute oral bioavailability was calculated with the AUC_{last} of IMQ IV bolus.

[b] One-way ANOVA followed by Dunnett's comparison was used for the statistical analysis of F_{oral} and $t_{1/2}$ of IMQ following administration of IMQ, prodrug 5 and prodrug 8. [ns] $p > 0.05$; *, $p < 0.05$.

administration of IMQ itself and IV administration of prodrugs 5 and 8, suggesting that the rate of IMQ release from prodrugs was slower than the rate of elimination of IMQ (Table 2). Additionally, the fraction of prodrugs converted to parent drugs was calculated using a previously reported equation (Shayeganpour et al., 2008). The calculations suggest that 52.0 % and 47.9 % of prodrug 5 and prodrug 8, respectively, were converted to IMQ following the IV administration of prodrugs (**Calculated fractions of prodrugs converted to parent drug**, **Supplementary material**).

Following oral administration of prodrugs 5 and 8, the T_{max} of prodrugs themselves was between 1–2 h (Table 3), while the T_{max} of IMQ was 2–6 h (Table 2). The plasma concentration–time profile of IMQ following oral administration of prodrugs 5 and 8 is neither erratic nor prolonged, as opposed to the oral administration of IMQ itself (Fig. 3 **B** vs. Fig. 4 **B and D**). There is no difference in the F_{oral} of IMQ between administrations of equimolar doses of the parent drug and prodrugs (Table 2).

3.5. Biodistribution of IMQ, prodrug 5 and prodrug 8

The BD of IMQ at apparent T_{max} points (1.5, 2, 6 and 28 h) following oral administration of unmodified IMQ with lipids is presented in Fig. 5. A high variability was observed in the concentrations of IMQ in all analysed tissues. As a result, the statistical analysis for most samples shows no statistically significant differences in the concentration of IMQ between tissues. The average concentration of IMQ in main organs (liver, kidney, spleen and brain) at early time points (1.5 h and 2 h) was 6 to 9-fold higher than the concentration of IMQ in plasma, indicating that IMQ rapidly and non-specifically distributes into organs and tissues.

Interestingly, although IMQ showed poor affinity to CM, the average concentrations of IMQ in mesenteric lymph nodes (MLNs) were 3.9-, 3.9-, 4.9- and 12-fold higher than the concentration of IMQ in plasma at 1.5 h, 2 h, 6 h and 28 h, respectively. Similarly, the average concentrations of IMQ in iliac lymph nodes (ILNs) were 4.5-, 4.7-, 3.1- and 3.0-fold higher than plasma at 1.5 h, 2 h, 6 h and 28 h, respectively. However, there is no difference between the concentration of IMQ in the mesenteric lymph fluid and plasma at 1.5 h and 2 h (Fig. 5). Fig. 6 demonstrates the concentration of IMQ in the intestinal contents. It indicates that IMQ was mainly found in the small intestine at 2 h time point following oral administration.

For assessment of intestinal lymphatic delivery of IMQ using prodrugs 5 and 8, biodistribution (BD) studies were conducted at 1.5 h and 6 h following an oral gavage of prodrugs. The selection of the time points was based on our previous works suggesting that when the intestinal lymphatic transport occurs, the concentration of drugs in the intestinal lymphatics could be highest at or just before the T_{max} in plasma (Lee et al., 2018; Qin et al., 2020). Fig. 7 **A** shows that substantial delivery of prodrug 5 to the mesenteric lymph was achieved with 50-fold higher average concentration of IMQ in the lymph fluid in comparison to plasma at 1.5 h. Similarly, the average concentrations of prodrug 8 in mesenteric lymph were 11-fold higher than in plasma at 1.5 h (Fig. 7 **C**).

At 1.5 h the concentration of active IMQ released from prodrug 5 in

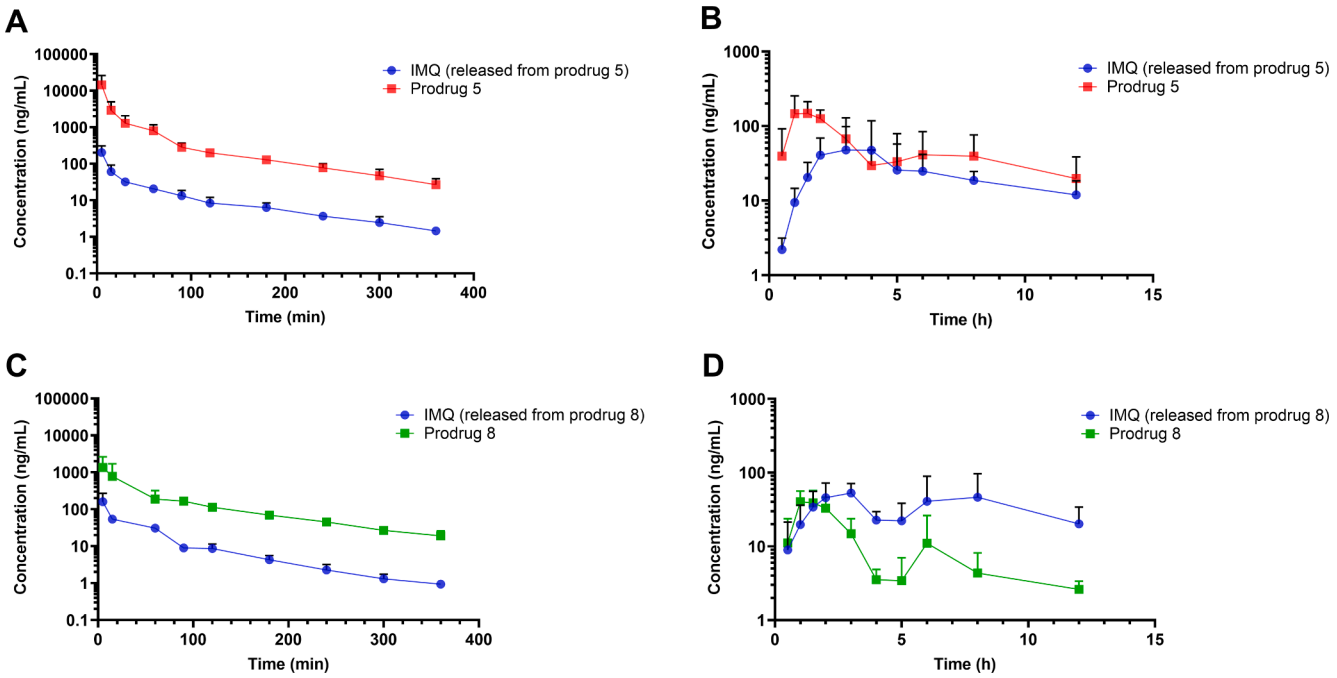

Fig. 4. Plasma concentration–time profiles of IMQ, prodrug 5, prodrug 8 and IMQ that was released from the prodrugs following: panel (A) IV bolus of prodrug 5 (1.49 mg/Kg, n = 4); panel (B) Oral administration of prodrug 5 in lipid-based formulation (14.9 mg/Kg, n = 6); panel (C) IV bolus of prodrug 8 (1.69 mg/Kg, n = 4); panel (D) Oral administration of prodrug 8 in lipid-based formulation (16.9 mg/Kg, n = 5) (mean ± SD).

Table 3
Pharmacokinetic parameters of prodrugs following administration of prodrug 5 (1.49 mg/kg for IV and 14.9 mg/kg for PO) and prodrug 8 (1.67 mg/kg for IV and 16.7 mg/Kg for PO) (n = 4 to 6). All data are shown as mean ± SD. An unpaired *t*-test was used to compare the V_{ss} of prodrugs 5 and 8 to the V_{ss} of IMQ.

Compound dose Administration route	Prodrug 5 IV	PO	Prodrug 8 IV	PO
AUC_{inf} (h·ng/mL)	5280.8 ± 3533.9	749.3 ± 520.9	1186.4 ± 602.1	143.1 ± 18.0
AUC_{last} (h·ng/mL)	5223.0 ± 3516.0	609.9 ± 286.7	1062.1 ± 614.3	129.6 ± 23.2
C_0 or C_{max} (ng/mL)	33102.0 ± 27251.7	185.3 ± 87.0	2882.2 ± 2564.6	51.8 ± 10.3
CL (mL/h/kg)	437.8 ± 327.1	–	1814.5 ± 683.1	–
V_{ss} (mL/kg)	443.9 ± 202.7[b] *	–	2241.7 ± 1221.3[b] ns	–
T_{max} (h)	–	1 - 2	–	1 - 2
$t_{1/2}$ (h)	1.4 ± 0.3	4.4 ± 3.1	1.4 ± 0.2	3.3 ± 1.2
F_{oral} (%)[a]	–	1.2 ± 0.8	–	1.3 ± 0.3

AUC_{inf} area under the curve from time zero to infinity; AUC_{last}, area under the curve from time zero to the last observed time point (0 – 360 min for IV administration of prodrugs; 0 – 12 h for PO administration of prodrugs); C_{max}, maximum observed concentration; C_0, concentration extrapolated to time zero; CL, clearance; V_{ss}, volume of distribution at steady state; T_{max} maximum concentration; $t_{1/2}$, half-life; F_{oral}, absolute oral bioavailability.

[a] The F_{oral} was calculated using the AUC_{last} of prodrugs following IV bolus.

[b] One-way ANOVA followed by Dunnett's comparison was used to compare the V_{ss} of prodrugs 5 and 8 to the V_{ss} of IMQ (in Table 2). Asterisks denote significance against the V_{ss} of IMQ. ns $p > 0.05$; *, $p < 0.05$.

MLNs was significantly higher than the concentration of IMQ in plasma (Fig. 8), indicating that prodrug 5 efficiently released IMQ in the intestinal lymphatic system. The tissue-to-plasma ratio of IMQ levels in the mesenteric lymph and MLNs was significantly increased from 0.5-fold to 1.9-fold and from 5-fold to 11-fold, respectively, following the oral administration of prodrug 5 (Fig. 9). A similar result was also found with the administration of prodrug 8 (Fig. 9). As opposed to MLNs, the tissue-to-plasma ratio of IMQ in the ILNs was similar following the administration of the prodrugs and unmodified IMQ.

As could be seen in Fig. 5, IMQ was widely distributed into highly blood-perfused organs, such as the spleen, liver and kidney, as well as relatively low blood-perfused organs, such as brain, following oral administration of IMQ itself. To understand if the distribution pattern of IMQ into organs was altered when prodrugs were administered, we compared the tissue-to-plasma ratio of IMQ in main organs following oral administration of IMQ and its prodrugs (Fig. 10). It was shown that with the oral administration of prodrug 5 in particular, the tissue-to-plasma ratio of IMQ was significantly decreased in comparison to the administration of unmodified IMQ and prodrug 8.

4. Discussion

In CRC patients, immature DCs can capture tumour-associated antigens (TAAs), inducing their maturation. Only mature DCs are able to present the TAAs through MHC II to naïve T cells in the tumour-draining lymph nodes (LNs), resulting in activation of the anti-cancer immune response (Miller et al., 2004; Wculek et al., 2020). The mesenteric lymph nodes (MLNs) and iliac lymph nodes (ILNs) are enriched in DCs and lymphocytes and drain the lymph from the colorectal regions (Kim et al., 2004; Sasaki et al., 2023; Shu et al., 2020; Yeo et al., 2010). Previously, it was suggested that the poor therapeutic outcomes of immunomodulators in CRC patients were associated with the suppression of DCs maturation in LNs, resulting in inhibition of activation of $CD8^+$ and $CD4^+$ T cells and also a reduction in T cell infiltration into tumour regions (Ciardiello et al., 2019; Dhodapkar et al., 2008; Gulubova et al., 2012; Kusume et al., 2009; McDonnell et al., 2010). IMQ is the only TRL7 agonist that is currently clinically approved for cancer treatment. It was shown that IMQ activates the DCs *via* the MyD88 signalling pathway, which results in the facilitation of the maturation of DCs and secretion of immunostimulatory signals (Patente et al., 2019; Wculek et al., 2020). Therefore, targeted delivery of IMQ to MLNs and ILNs has potential to facilitate the maturation of DCs and stimulate the anti-tumour immune response, overcoming the immune suppression and eventually improving the treatment outcomes for CRC patients.

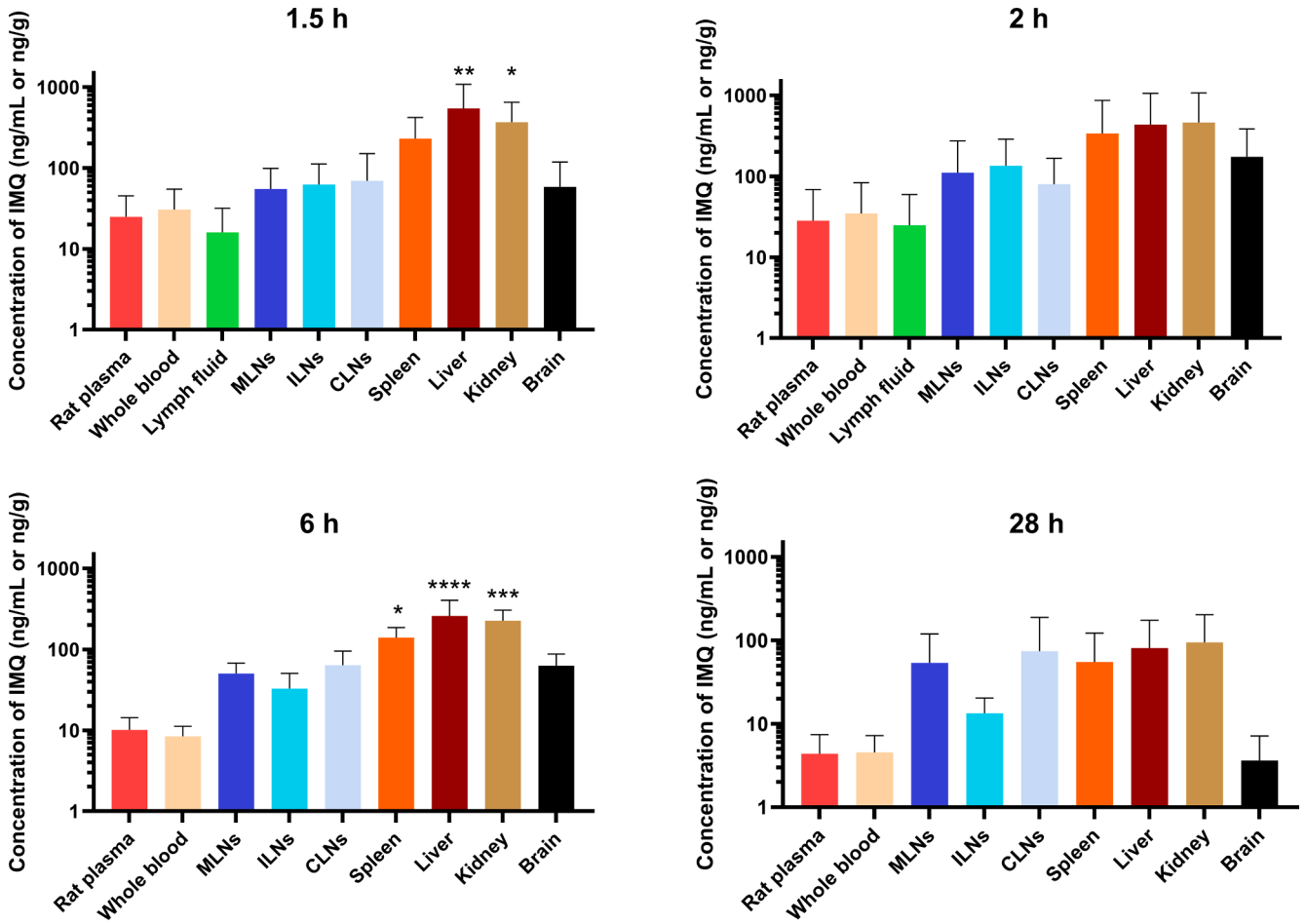

Fig. 5. The biodistribution of IMQ following oral administration of IMQ (8 mg/kg) with lipids at local T_{max} 1.5 h, 2 h, 6 h and 28 h (mean ± SD, n = 4 to 6). MLN, mesenteric lymph node; ILNs, iliac lymph nodes; CLNs, cervical lymph nodes. One-way ANOVA, followed by Dunnett's comparison, was used for statistical analysis. Asterisks denote statistical significance against plasma. *, $p < 0.05$; **,$p < 0.01$, ***,$p < 0.001$ ****,$p < 0.0001$.

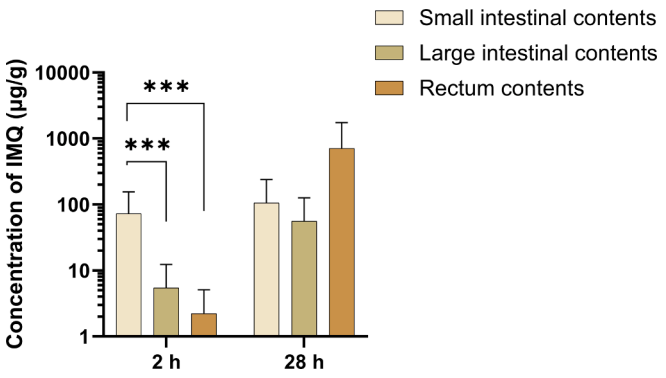

Fig. 6. The concentration of IMQ in the intestinal contents at local T_{max} 2 h and 28 h. One-way ANOVA followed by Tukey's comparison was used for statistical analysis. ***,$p < 0.001$.

Therefore, in this work, the approach of highly lipophilic amide prodrugs of IMQ in combination with LCT formulation was utilised to deliver IMQ specifically into the intestinal lymphatics following oral administration.

4.1. Pharmacokinetics and biodistribution of IMQ

It was reported in the past that the oral bioavailability (F_{oral}) of IMQ in rats was essentially zero (Wang, 2010). However, in the current study, it was found that the F_{oral} of IMQ in rats was indeed limited (< 10 %) but not zero (Table 2). The concentration–time profile of IMQ after oral administration shows that the absorption of IMQ was prolonged and erratic (Fig. 3). We hypothesised that this prolonged absorption profile is related to the dissolution and precipitation cycles of IMQ in the different regions in the GI tracts, leading to multiple absorption windows. In this study, IMQ was prepared in an acidic formulation (0.05 N HCl) to facilitate its dissolution. In the first two hours after oral administration, a relatively rapid increase in IMQ concentration in plasma was observed, indicating absorption from the upper GI tract. However, with an increase in pH in the lower parts of the small intestine, IMQ probably precipitated, resulting in limited absorption from these regions (McConnell et al., 2010). The second relatively rapid increase in IMQ concentrations was observed as late as 20 h after administration. At this stage, the remaining IMQ in the GI tract would likely be already in the lowest parts of the colon and rectum, and the peak could reflect the absorption from this area, which partially avoids hepatic first-pass metabolism (Washington et al., 2000). This hypothesis was investigated by assessing the concentration of IMQ in the intestinal contents at 2 h and 28 h, which were considered as two of the apparent T_{max} points of IMQ following oral administration (Fig. 6). It was shown that IMQ was mainly found in the small intestine at 2 h, and a substantial amount of IMQ was trapped within the intestinal lumen up to 28 h.

IMQ has a very low affinity to artificial CMs and limited triglyceride solubility (Table 1), indicating a low intestinal lymphatic transport potential by the CM association pathway. Surprisingly, the biodistribution study of IMQ following oral administration showed substantial levels of

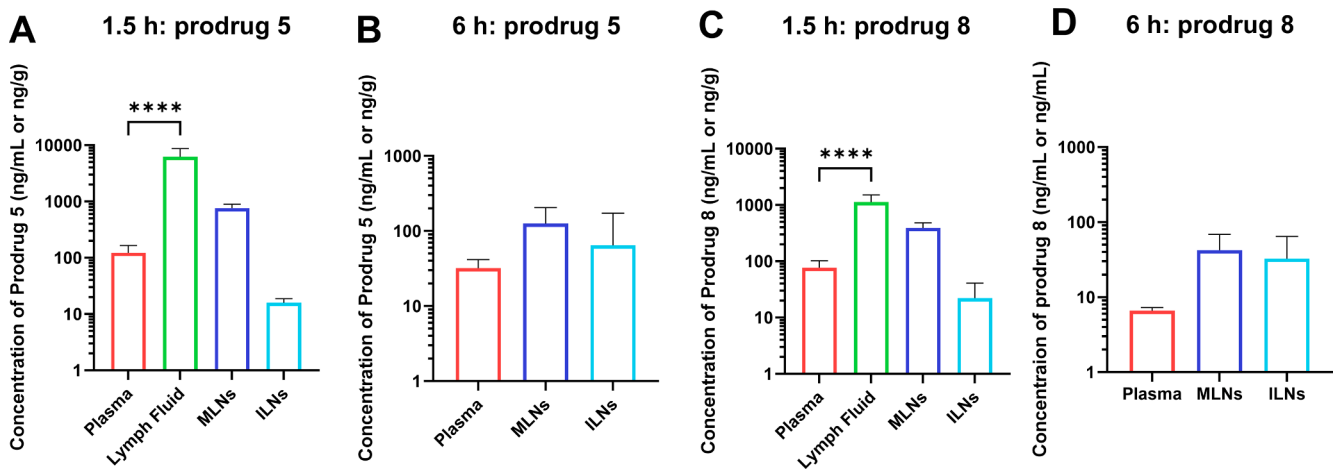

Fig. 7. The biodistribution of prodrugs 5 and 8 in plasma, mesenteric lymph, mesenteric lymph nodes (MLNs) and iliac lymph nodes (ILNs) (mean ± SD, n = 4 to 8). Panels A and B show the distribution of prodrug 5 (14.9 mg/kg) following oral administration at 1.5 and 6 h, respectively. Panels C and D show the distribution of prodrug 8 (16.7 mg/kg) following oral administration at 1.5 and 6 h, respectively. One-way ANOVA, followed by Dunnett's comparison, was used for statistical analysis. Asterisks denote statistical significance against plasma. ****,$p < 0.0001$.

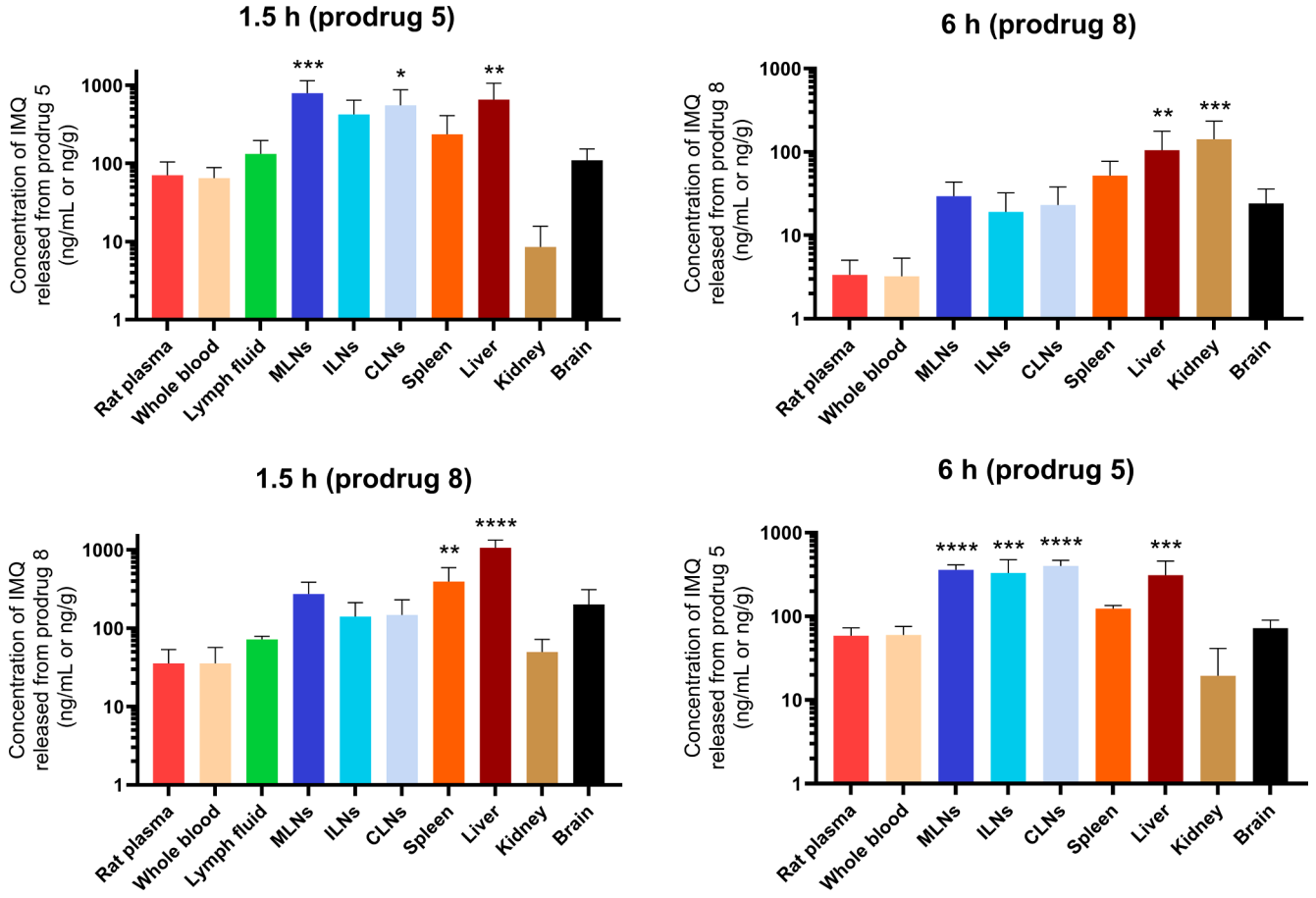

Fig. 8. The distribution of IMQ in plasma, mesenteric lymph fluid, lymph nodes and main organs following oral administrations of prodrug 5 (14.9 mg/kg) and 8 (16.7 mg/kg) using lipid-based formulation at 1.5 and 6 h (mean ± SD, n = 5 to 8). MLN, mesenteric lymph node; ILNs, iliac lymph nodes; CLNs, cervical lymph nodes. One-way ANOVA, followed by Dunnett's comparison, was used for statistical analysis. Asterisks denote statistical significance against plasma. *$p < 0.05$; **,$p < 0.01$, ***,$p < 0.001$, ****,$p < 0.0001$.

the drug in mesenteric lymph nodes (MLNs) and iliac lymph nodes (ILNs) (Fig. 5), which drain lymph from the duodenum, small intestine, cecum, colon, and rectum (Tilney, 1971). However, there was no statistically significant difference between concentrations of IMQ in plasma and mesenteric lymph fluid at 1.5 h and 2 h (Fig. 5), suggesting that the accumulation of IMQ in MLNs and ILNs was probably not a result of intestinal lymphatic transport. In addition, there was a clear trend that IMQ was highly distributed into cervical lymph nodes (CLNs) and various organs (spleen, liver, kidney and brain) (Fig. 5). With non-compartmental PK analysis, it was shown that the apparent volume of

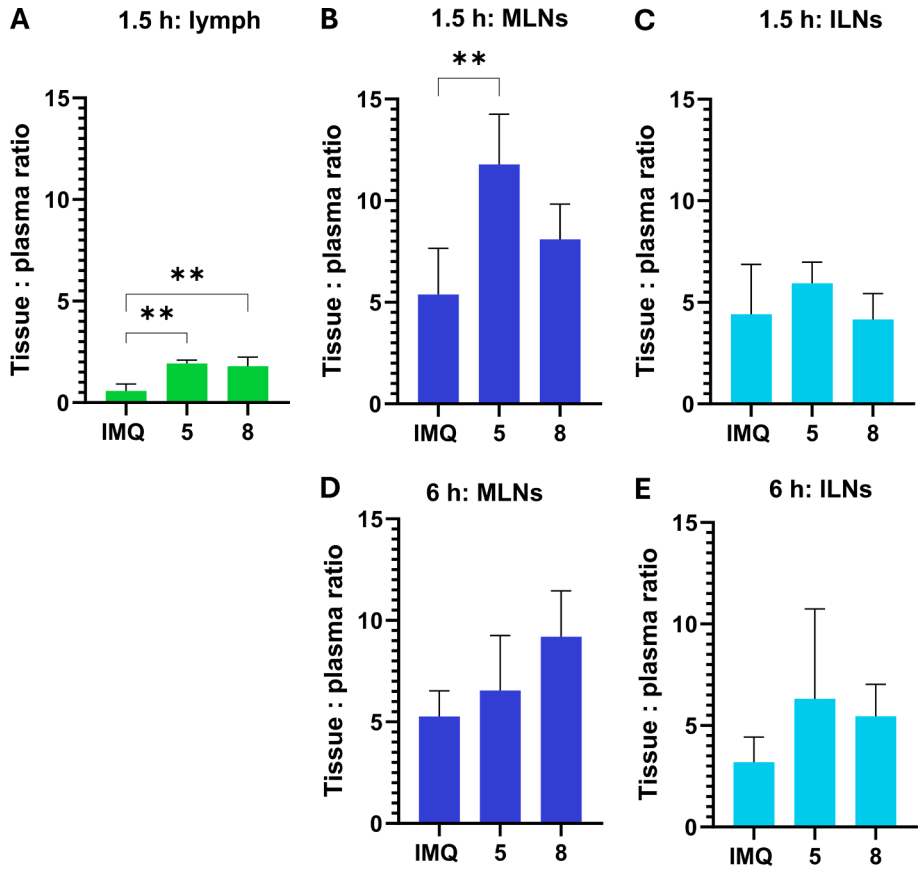

Fig. 9. The ratios of distribution of IMQ into panel (A) mesenteric lymph, panel (B) mesenteric lymph nodes (MLNs) and panel (C) iliac lymph nodes (ILNs) following oral administration of IMQ (8 mg/kg) with lipid, prodrug 5 (14.9 mg/kg) and prodrug 8 (16.7 mg/kg). All results are presented as mean ± SD (n = 4 to 8). One-way ANOVA, followed by Dunnett's comparison, was used for statistical analysis. **, p < 0.01*.

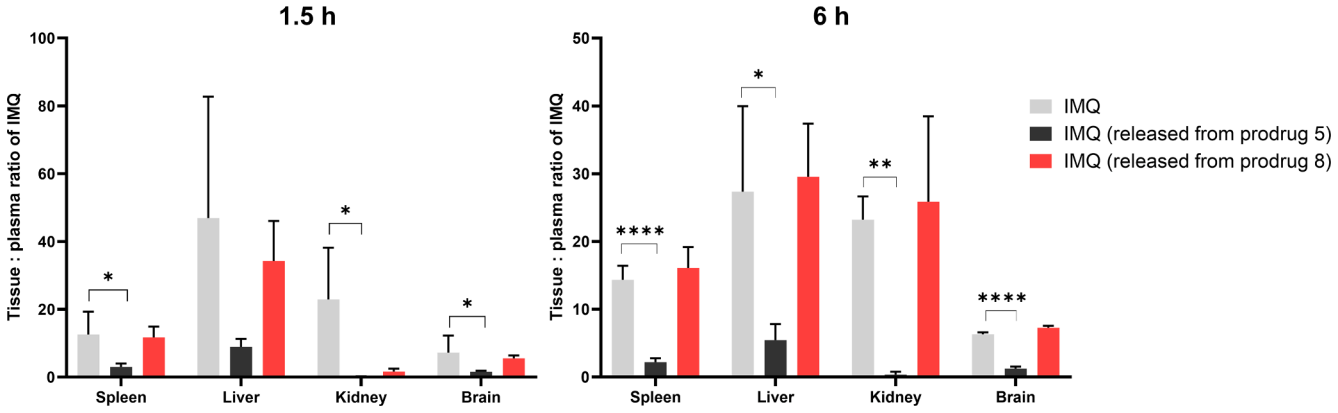

Fig. 10. The distribution of IMQ into the spleen, liver, kidney and brain following oral administration of unmodified IMQ (8 mg/kg) with lipids, prodrug 5 (14.9 mg/kg) and prodrug 8 (16.7 mg/kg) at 1.5 h and 6 h. Results are presented as the ratio of IMQ concentration in the analysed sample to IMQ concentration in plasma. All results are presented as mean ± SD (n = 4 to 8). One-way ANOVA, followed by Dunnett's comparison, was used for statistical analysis. Asterisks denote statistical significance against unmodified IMQ group **, p < 0.05; **,p < 0.01; ****,p < 0.0001*.

distribution (V_{ss}) of IMQ is quite high (3376.3 ± 1842.0 mL/kg) (Table 2). We have also assessed the V_{ss} of IMQ following IV administration using data published in previous literature (Falke et al., 2018; Kang et al., 2019). Results showed this high V_{ss} found in our study is consistent with previous studies (7295.8 mL/Kg and 6784.3 mL/Kg). This high V_{ss} suggests that the high amount of IMQ found in LNs was, at least partially, due to a non-specific distribution of IMQ to tissues. The high non-specific distribution of IMQ to organs and tissues can contribute to its systemic adverse effects and toxicity. Therefore, highly lipophilic prodrugs of IMQ were designed to improve the targeted delivery of IMQ to the intestinal lymphatics.

4.2. The potential of intestinal lymphatic transport of IMQ prodrugs

It has been shown previously that the main predictor for intestinal lymphatic transport of a molecule is its affinity to CMs (Gershkovich and Hoffman, 2005). The affinity of IMQ prodrugs to CMs was substantially higher than that of IMQ (which was undetectable) (Table 1). Previously,

Chu *et al.* suggested that the degree of unsaturation of the conjugated fatty acid could facilitate the affinity of prodrugs to CMs (Chu et al., 2023). In this study, we observed a similar trend (prodrug 4 vs. prodrugs 7 and 8); however, no statistically significant difference was found (Table 1). In addition to the CMs affinity, the high solubility in long-chain triglycerides (LCT) (> 50 mg/mL) is another important predictor for intestinal lymphatic transport (Charman and Stella, 1986; Gershkovich et al., 2008). Combined LCT solubility and CM affinity results suggest that prodrugs 3–8 have a high potential to be transported into the intestinal lymphatics following oral administration (Table 1) (Chu et al., 2023).

4.3. The biotransformation and stability of IMQ prodrugs in biorelevant media

The rate of IMQ released from the prodrug in tested media directly corresponded to the hydrolysis half-life of prodrugs (Fig. 2), suggesting that the hydrolysis of the amide bond was the primary metabolic pathway of IMQ amide prodrugs in the tested conditions. For effective delivery of the active drug to the intestinal lymphatics, prodrug candidates should resist enzymatic hydrolysis in the gastrointestinal (GI) tract but quickly release IMQ once they enter the lymphatic system. The FaSSIF + esterase media and rat plasma were previously used to estimate the hydrolysis of the ester prodrugs in the GI lumen and lymph, respectively (Chu et al., 2023; Lee et al., 2018; Qin et al., 2020). It was found that, except prodrug 4, synthesised amide prodrugs efficiently released IMQ in the FaSSIF + esterase medium and rat plasma, suggesting an efficient hydrolysis of the amide bond (Fig. 2). Previously, a lipidised IMQ prodrug was synthesized by conjugating IMQ with cholesterol *via* an amide bond. It was observed that this IMQ-cholesterol prodrug can efficiently release the active molecule in a PBS/DMSO mixture (Yin et al., 2023). It was suggested that the hydrolysis of the amide bond in the IMQ prodrug can easily happen even without the presence of hydrolase. However, one of the well-known challenges for amide prodrugs is that the amide bond is substantially more stable than ester (Han et al., 2014; Han et al., 2021; Simplício et al., 2008). Therefore, we hypothesised that the rapid release of IMQ from prodrugs is related to its unique chemical structure and its properties as a leaving group. The amine in the IMQ is not an electrophile amine but an aniline. The electronic resonance could facilitate the release of IMQ, resulting in rapid hydrolysis of IMQ prodrugs.

In addition, it was noted that with an increase in the length of the alkyl chain (prodrugs 1–4), the half-lives of prodrugs in FaSSIF with added esterase activity and rat plasma were also increased, most likely due to steric hindrance (Burke et al., 1997; Redden et al., 1999). Therefore, IMQ amide prodrugs 5–8 were designed as conjugates with unsaturated fatty acids to minimise steric hindrance. As expected, the introduction of unsaturation to prodrugs resulted in a faster conversion to active moiety.

To evaluate the biotransformation of IMQ amide prodrugs in the GI tract more accurately, in this work, the BBMVs medium was also evaluated for assessment of the hydrolysis of amide prodrugs. BBMVs are vesicles located in the apical side of enterocytes of the intestinal lumen (McConnell et al., 2009). These vesicles are enriched in metabolic enzymes, including alkaline phosphodiesterase, aminopeptidase and carboxypeptidase (Hooton et al., 2015). It has been used in the past for assessing peptide stability during GI absorption (Hess et al., 2007; Schumacher-Klinger et al., 2018). Brush border membrane could be one of the primary hydrolysis sites for amide prodrugs *in vivo*. The biotransformation assessment using BBMVs showed that all prodrugs were quite stable (Fig. 2), suggesting that designed prodrugs are likely to be resistant to hydrolysis, especially near and in the enterocytes, before entering the intestinal lymphatics. Taken together, the results of CM affinity, LCT solubility, biotransformation and stability, prodrugs 5 and 8, were selected as the most promising candidates for delivering IMQ into mesenteric and retroperitoneal lymphatics *via* the CM pathway.

4.4. Pharmacokinetics of IMQ and prodrugs 5 and 8

It was shown previously that the lipophilic prodrug approach combined with a lipid-based formulation could increase the F_{oral} of drugs (Lee et al., 2018; Nebaihi et al., 2023; Qin et al., 2020). However, in this work, there was no statistically significant difference in the F_{oral} of IMQ between the administration of unmodified IMQ and the administration of prodrugs 5 and 8 (Table 2). The plasma concentration–time profile of IMQ following oral administration of prodrugs 5 and 8 was not prolonged and erratic as was the case for unmodified IMQ (Fig. 4). Therefore, we hypothesised that prodrugs 5 and 8 did not increase the extent of IMQ absorption but potentially changed the absorption pattern and pathway. To test this hypothesis, the biodistribution of prodrug 5, prodrug 8 and IMQ released from the prodrugs was assessed following oral administration of prodrugs 5 and 8. Prodrugs 5 and 8 have significantly higher affinity to CMs than unmodified IMQ (Table 1). As a result, high concentrations of prodrugs 5 and 8 were found in mesenteric lymph, strongly suggesting that the affinities of prodrugs 5 and 8 to CMs (70.3 % and 76.5 %, respectively) were sufficient for the substantial lymphatic uptake to occur *in vivo* (Fig. 7 **A** and **C**). It should be mentioned that the amine group on the 4-position of IMQ is an essential functional group responsible for its pharmacological effect. Therefore, although the off-target distribution of prodrugs could not be completely excluded (**Figure S8**, **Supplementary material**), the amidation of the amine on the 4-position with alkyl chains is unlikely to increase the toxicity of IMQ (Yin et al., 2023).

It should be noted that previously reported lipophilic prodrugs designed by us and others for intestinal lymphatics targeting mainly used an ester bond to conjugate active moiety with lipophilic structures (Amory et al., 2003; Chu et al., 2023; Han et al., 2014; Hu et al., 2016; Lee et al., 2018; Qin et al., 2020). To the best of our knowledge, only one work by Han *et al.* has previously attempted to design lipophilic prodrugs for targeting intestinal lymphatics through an amide bond (Han et al., 2014). The authors reported that the amide lipophilic prodrug approach did not improve intestinal lymphatic targeting due to insufficient release of the active drug within the mesenteric lymph (Han et al., 2014). However, in the current study, a significant increase in the lymph-to-plasma concentration ratio of IMQ was observed when prodrugs were administered, in comparison to the administration of the unmodified IMQ (Fig. 9 **A**). Moreover, a substantial increase was found in the MLNs-to-plasma concentration ratio of IMQ from 5.3-fold to 11.8-fold with prodrug 5 ($p = 0.0029$) and to 8.0-fold with prodrug 8 ($p = 0.079$) in comparison to unmodified IMQ (Fig. 9 **B**). Most importantly, following oral administration of prodrug 5, IMQ concentrations in MLNs were significantly higher than in plasma, indicating that IMQ was targeted into intestinal LNs (Fig. 8).

However, as opposed to prodrug 5, IMQ concentrations in MLNs were not significantly higher than in plasma following the administration of prodrug 8 and unmodified IMQ. Additionally, prodrug 5 achieved a higher concentration of IMQ in MLNs and a higher MLNs-to-plasma ratio in comparison to prodrug 8 (Fig. 8 **and** Fig. 9 **B**). This is probably because the lymphatic delivery of prodrug 8 was lower than that of prodrug 5 (Fig. 7 **A** and **C**) and the biotransformation of prodrug 8 to IMQ in intestinal lymphatics was slower than that of prodrug 5 (Fig. 2).

It is important to note that MLNs are important targets for immune activators, such as toll-like receptor 7 (TLR 7) agonists. These lymph nodes are rich in DCs that are derived from the primary lymphoid tissues and DCs that migrate from the intestinal tissue, as well as naïve T cells, providing an environment for immune cells cross-communication in CRC patients (Houston et al., 2016). The concentration of IMQ in MLNs is 1.6-fold higher than its EC_{50} (around 2 μM) as a TLR7 agonist, suggesting that targeted delivery IMQ to MLNs using prodrug 5 can potentially improve the treatment for CRC (Shukla et al., 2010).

Concerning ILNs targeting, results suggest that following oral administration of prodrug 5, IMQ concentrations in ILNs were significantly higher in comparison to oral administration of unmodified IMQ

(**Figure S9**, **Supplementary material**). However, the ILNs-to-plasma concentration ratio of IMQ was not significantly different between oral administration of unmodified IMQ and prodrugs (Fig. 9 **C**). This could suggest that the increase in the IMQ concentrations in ILNs may be not a direct result of intestinal lymphatic transport.

Additionally, compared to the V_{ss} of IMQ (3376.3 ± 1842.0 mL/kg) (Table 2), a lower V_{ss} of prodrug 5 (443.9 ± 202.7 mL/kg, $p < 0.05$) and the V_{ss} of prodrug 8 (2241.7 ± 1221.3 mL/kg, $p > 0.05$) was found (Table 3). As a result, when prodrug 5 was administered, this non-specific distribution of IMQ was reduced (Fig. 10), suggesting that the off-target toxicity of IMQ could be potentially reduced using the prodrug approach.

5. Conclusion

In this study, lipophilic amide prodrugs were designed and assessed for their potential for intestinal transport and targeting of active IMQ into mesenteric and retroperitoneal lymph nodes following oral administration *via* the CMs pathway. In the design and *in vitro* assessment for prodrugs, we found that: 1) conjugation with a linear alkyl chain resulted in a substantial affinity of prodrugs to artificial CM; 2) inclusion of unsaturated bonds in the alkyl chain facilitated the active moiety released from amide prodrugs. Prodrugs 5 and 8 were selected as the most promising candidates and, therefore, were orally administered to rats. They were efficiently delivered to mesenteric lymphatics and released active IMQ in mesenteric lymph and lymph nodes. This work suggests that the approach of targeting IMQ to the mesenteric lymphatic system using lipophilic amide prodrugs is efficient. This study demonstrates more generally that the lipophilic amide prodrug approach for amine molecules for intestinal lymphatic targeting is feasible.

CRediT authorship contribution statement

Haojie Chen: Conceptualization, Methodology, Software, Validation, Formal analysis, Writing – original draft. **Liuhang Ji:** Investigation. **Abigail Wong:** Writing – review & editing, Investigation. **Yenju Chu:** Methodology, Investigation. **Wanshan Feng:** Methodology, Investigation. **Yufei Zhu:** Investigation. **Junting Wang:** Investigation. **Eleonora Comeo:** Methodology, Investigation. **Dong-Hyun Kim:** Writing – review & editing, Supervision. **Michael J. Stocks:** Writing – review & editing, Supervision. **Pavel Gershkovich:** Conceptualization, Methodology, Supervision, Resources, Project administration, Writing – review & editing.

Declaration of competing interest

The authors declare that they have no known competing financial interests or personal relationships that could have appeared to influence the work reported in this paper.

Appendix A. Supplementary data

Supplementary data to this article can be found online at https://doi.org/10.1016/j.ijpharm.2024.124895.

Data availability

Data will be made available on request.

References

Amory, J.K., Scriba, G.K.E., Amory, D.W., Bremner, W.J., 2003. Oral Testosterone-Triglyceride Conjugate in Rabbits: Single-Dose Pharmacokinetics and Comparison with Oral Testosterone Undecanoate. J. Androl. 24 (5), 716–720. https://doi.org/10.1002/j.1939-4640.2003.tb02732.x.

Bai, L., Li, W., Zheng, W., Dongsheng, Xu., Chen, N., Cui, J., 2020. Promising Targets Based on Pattern Recognition Receptors for Cancer Immunotherapy. Pharmacol. Res. 159 (June), 105017. https://doi.org/10.1016/j.phrs.2020.105017.

Bai, H., Wang, Z., Li, M., Sun, P., Wei, S., Wang, W., Wang, Z., Xing, Y., Li, J., Dardik, A., 2021. Inhibition of Programmed Death-1 Decreases Neointimal Hyperplasia after Patch Angioplasty. J. Biomed. Mater. Res. B Appl. Biomater. 109 (2), 269–278. https://doi.org/10.1002/jbm.b.34698.

Beutner, G.L., Young, I.S., Davies, M.L., Hickey, M.R., Park, H., Stevens, J.M., Ye, Q., 2018. TCFH-NMI: Direct Access to N-Acyl Imidazoliums for Challenging Amide Bond Formations. Org. Lett. 20 (14), 4218–4222. https://doi.org/10.1021/acs.orglett.8b01591.

Buchbinder, E.I., Desai, A., 2016. CTLA-4 and PD-1 Pathways Similarities, Differences, and Implications of Their Inhibition. American Journal of Clinical Oncology: Cancer Clinical Trials 39 (1), 98–106. https://doi.org/10.1097/COC.0000000000000239.

Burke, Michael, Peter R. Redden, Jo-Anne Douglas, Arthur Dick, and David F. Horrobin. 1997. *In Vitro Hydrolysis of Novel Gamma-Linolenoyloxyalkyl Derivatives of Theophylline*. Vol. 157.

Charman, W. N. A., and V. J. Stella. 1986. *Estimating the Maximal Potential for Intestinal Lymphatic Transport of Lipophilic Drug Molecules*. Vol. 34.

Chu, Yenju, Chaolong Qin, Wanshan Feng, Charles Sheriston, Yu Jane Khor, Concepción Medrano-Padial, Birgit E. Watson, Teddy Chan, Binhua Ling, Michael J. Stocks, Peter M. Fischer, and Pavel Gershkovich. 2021. "Oral Administration of Tipranavir with Long-Chain Triglyceride Results in Moderate Intestinal Lymph Targeting but No Efficient Delivery to HIV-1 Reservoir in Mesenteric Lymph Nodes." *International Journal of Pharmaceutics* 602(November 2020). doi: 10.1016/j.ijpharm.2021.120621.

Chu, Y., Wong, A., Chen, H., Ji, L., Qin, C., Feng, W., Stocks, M.J., Gershkovich, P., 2023. Development of Lipophilic Ester Prodrugs of Dolutegravir for Intestinal Lymphatic Transport. Eur. J. Pharm. Biopharm. 191, 90–102. https://doi.org/10.1016/j.ejpb.2023.08.015.

Ciardiello, D., Vitiello, P.P., Cardone, C., Martini, G., Troiani, T., Martinelli, E., Ciardiello, F., 2019. Immunotherapy of Colorectal Cancer: Challenges for Therapeutic Efficacy. Cancer Treat. Rev. 76, 22–32.

Dhodapkar, M.V., Dhodapkar, K.M., Palucka, A.K., 2008. Interactions of Tumor Cells with Dendritic Cells: Balancing Immunity and Tolerance. Cell Death Differ. 15 (1), 39–50.

Dudek, A.Z., Yunis, C., Harrison, L.I., Kumar, S., Hawkinson, R., Cooley, S., Vasilakos, J. P., Gorski, K.S., Miller, J.S., 2007. First in Human Phase I Trial of 852A, a Novel Systemic Toll-like Receptor 7 Agonist, to Activate Innate Immune Responses in Patients with Advanced Cancer. Clin. Cancer Res. 13 (23), 7119–7125. https://doi.org/10.1158/1078-0432.CCR-07-1443.

Falke, J., Christina, A., de Kaa, H.-V., Maj, R., Oosterwijk, E., Witjes, J.A., 2018. Pharmacokinetics and Pharmacodynamics of Intravesical and Intravenous TMX-101 and TMX-202 in a F344 Rat Model. Urologic Oncology: Seminars and Original Investigations 36 (5), 242.e1–242.e7. https://doi.org/10.1016/j.urolonc.2018.01.016.

Fanous, M.Y.Z., Phillips, A.J., Windsor, J.A., 2007. Mesenteric Lymph: The Bridge to Future Management of Critical Illness. Journal of the Pancreas 8 (4), 374–399.

Feng, W., Qin, C., Chu, Y.J., Berton, M., Lee, J.B., Zgair, A., Bettonte, S., Stocks, M.J., Constantinescu, C.S., Barrett, D.A., Fischer, P.M., Gershkovich, P., 2021a. Natural Sesame Oil Is Superior to Pre-Digested Lipid Formulations and Purified Triglycerides in Promoting the Intestinal Lymphatic Transport and Systemic Bioavailability of Cannabidiol. Eur. J. Pharm. Biopharm. 162, 43–49. https://doi.org/10.1016/j.ejpb.2021.02.013.

Feng, W., Qin, C., Chu, Y.J., Berton, M., Lee, J.B., Zgair, A., Bettonte, S., Stocks, M.J., Constantinescu, C.S., Barrett, D.A., Fischer, P.M., Gershkovich, P., 2021b. Natural Sesame Oil Is Superior to Pre-Digested Lipid Formulations and Purified Triglycerides in Promoting the Intestinal Lymphatic Transport and Systemic Bioavailability of Cannabidiol. Eur. J. Pharm. Biopharm. 162 (January), 43–49. https://doi.org/10.1016/j.ejpb.2021.02.013.

Frega, Giorgio, Qi Wu, Julie Le Naour, Erika Vacchelli, Lorenzo Galluzzi, Guido Kroemer, and Oliver Kepp. 2020. "Trial Watch: Experimental TLR7/TLR8 Agonists for Oncological Indications." *OncoImmunology* 9(1). doi: 10.1080/2162402X.2020.1796002.

Ganesan, A., Ahmed, M., Okoye, I., Arutyunova, E., Babu, D., Turnbull, W.L., Kundu, J. K., Shields, J., Agopsowicz, K.C., Lai, Xu., Tabana, Y., Srivastava, N., Zhang, G., Moon, T.C., Belovodskiy, A., Hena, M., Kandadai, A.S., Hosseini, S.N., Hitt, M., Walker, J., Smylie, M., West, F.G., Siraki, A.G., Joanne Lemieux, M., Elahi, S., Nieman, J.A., Lorne Tyrrell, D., Houghton, M., Barakat, K., 2019. Comprehensive in Vitro Characterization of PD-L1 Small Molecule Inhibitors. Sci. Rep. 9 (1), 12392. https://doi.org/10.1038/s41598-019-48826-6.

Gershkovich, P., Fanous, J., Qadri, B., Yacovan, A., Amselem, S., Hoffman, A., 2008. The Role of Molecular Physicochemical Properties and Apolipoproteins in Association of Drugs with Triglyceride-Rich Lipoproteins: In-Silico Prediction of Uptake by Chylomicrons. J. Pharm. Pharmacol. 61 (1), 31–39. https://doi.org/10.1211/jpp/61.01.0005.

Gershkovich, P., Hoffman, A., 2005. Uptake of Lipophilic Drugs by Plasma Derived Isolated Chylomicrons: Linear Correlation with Intestinal Lymphatic Bioavailability. Eur. J. Pharm. Sci. 26 (5), 394–404. https://doi.org/10.1016/j.ejps.2005.07.011.

Gulubova, M.V., Ananiev, J.R., Vlaykova, T.I., Yovchev, Y., Tsoneva, V., Manolova, I.M., 2012. Role of Dendritic Cells in Progression and Clinical Outcome of Colon Cancer. Int. J. Colorectal Dis. 27 (2), 159–169. https://doi.org/10.1007/s00384-011-1334-1.

Han, S., Quach, T., Luojuan, Hu., Wahab, A., Charman, W.N., Stella, V.J., Trevaskis, N.L., Simpson, J.S., Porter, C.J.H., 2014. Targeted Delivery of a Model Immunomodulator to the Lymphatic System: Comparison of Alkyl Ester versus Triglyceride Mimetic

Lipid Prodrug Strategies. J. Control. Release 177 (1), 1–10. https://doi.org/10.1016/j.jconrel.2013.12.031.
Han, S., Quach, T., Luojuan, Hu., Lim, S.F., Gracia, G., Trevaskis, N.L., Simpson, J.S., Porter, C.J.H., 2021. The Impact of Conjugation Position and Linker Chemistry on the Lymphatic Transport of a Series of Glyceride and Phospholipid Mimetic Prodrugs. J. Pharm. Sci. 110 (1), 489–499. https://doi.org/10.1016/j.xphs.2020.10.021.
Hess, S., Ovadia, O., Shalev, D.E., Senderovich, H., Qadri, B., Yehezkel, T., Salitra, Y., Sheynis, T., Jelinek, R., Gilon, C., Hoffman, A., 2007. Effect of Structural and Conformation Modifications, Including Backbone Cyclization, of Hydrophilic Hexapeptides on Their Intestinal Permeability and Enzymatic Stability. J. Med. Chem. 50 (24), 6201–6211. https://doi.org/10.1021/jm070836d.
Hooton, D., Lentle, R., Monro, J., Wickham, M., Simpson, R., 2015. The Secretion and Action of Brush Border Enzymes in the Mammalian Small Intestine. Rev. Physiol. Biochem. Pharmacol. 168, 59–118. https://doi.org/10.1007/112_2015_24.
Houston, S.A., Cerovic, V., Thomson, C., Brewer, J., Mowat, A.M., Milling, S., 2016. The Lymph Nodes Draining the Small Intestine and Colon Are Anatomically Separate and Immunologically Distinct. Mucosal Immunol. 9 (2), 468–478. https://doi.org/10.1038/mi.2015.77.
Hu, L., Quach, T., Han, S., Lim, S.F., Yadav, P., Senyschyn, D., Trevaskis, N.L., Simpson, J.S., Porter, C.J.H., 2016. Glyceride-Mimetic Prodrugs Incorporating Self-Immolative Spacers Promote Lymphatic Transport, Avoid First-Pass Metabolism, and Enhance Oral Bioavailability. Angew. Chem. 128 (44), 13904–13909. https://doi.org/10.1002/ange.201604207.
Jia, L., Liu, K., Fei, T., Liu, Q., Zhao, X., Hou, L., Zhang, W., 2021. Programmed Cell Death–1/Programmed Cell Death–ligand 1 Inhibitors Exert Antiapoptosis and Antiinflammatory Activity in Lipopolysaccharide Stimulated Murine Alveolar Macrophages. Exp. Ther. Med. 21 (4), 400. https://doi.org/10.3892/etm.2021.9831.
Kang, T., Li, Y., Wang, Y., Zhu, J., Yang, L., Huang, Y., Xiong, M., Liu, J., Wang, S., Huang, M., Wei, X., Gou, M., 2019. Modular Engineering of Targeted Dual-Drug Nanoassemblies for Cancer Chemoimmunotherapy. ACS Appl. Mater. Interfaces 11 (40), 36371–36382. https://doi.org/10.1021/acsami.9b11881.
Kesler, C.T., Liao, S., Munn, L.L., Padera, T.P., 2013. Lymphatic Vessels in Health and Disease. Wiley Interdiscip. Rev. Syst. Biol. Med. 5 (1), 111–124. https://doi.org/10.1002/wsbm.1201.
Kessler, M., Acuto, O., Storelli, C., Murer, H., Müller, M., Semenza, G., 1978. A modified procedure for the rapid preparation of efficiently transporting vesicles from small intestinal brush border membranes their. BBA 506 (1), 136–154.
Kim, J.C., Lee, K.H., Yu, C.S., Kim, H.C., Chang, H.M., Kim, J.H., Kim, J.S., Kim, T.W., 2004. The Clinicopathological Significance of Inferior Mesentric Lymph Node Metastasis in Colorectal Cancer. Eur. J. Surg. Oncol. 30 (3), 271–279. https://doi.org/10.1016/j.ejso.2003.12.002.
Kochappan, R., Cao, E., Han, S., Luojuan, Hu., Quach, T., Senyschyn, D., Ferreira, V.I., Lee, G., Leong, N., Sharma, G., Lim, S.F., Nowell, C.J., Chen, Z., von Andrian, U.H., Bonner, D., Mintern, J.D., Simpson, J.S., Trevaskis, N.L., Porter, C.J.H., 2021. Targeted Delivery of Mycophenolic Acid to the Mesenteric Lymph Node Using a Triglyceride Mimetic Prodrug Approach Enhances Gut-Specific Immunomodulation in Mice. J. Control. Release 332, 636–651. https://doi.org/10.1016/j.jconrel.2021.02.008.
Kusume, A., Sasahira, T., Luo, Y.i., Isobe, M., Nakagawa, N., Tatsumoto, N., Fujii, K., Ohmori, H., Kuniyasu, H., 2009. Suppression of Dendritic Cells by HMGB1 Is Associated with Lymph Node Metastasis of Human Colon Cancer. Pathobiology 76 (4), 155–162. https://doi.org/10.1159/000218331.
Lee, J.B., Zgair, A., Malec, J., Kim, T.H., Kim, M.G., Ali, J., Qin, C., Feng, W., Chiang, M., Gao, X., Voronin, G., Garces, A.E., Lau, C.L., Chan, T.H., Hume, A., McIntosh, T.M., Soukarieh, F., Al-Hayali, M., Cipolla, E., Collins, H.M., Heery, D.M., Shin, B.S., Yoo, S.D., Kagan, L., Stocks, M.J., Bradshaw, T.D., Fischer, P.M., Gershkovich, P., 2018. Lipophilic Activated Ester Prodrug Approach for Drug Delivery to the Intestinal Lymphatic System. J. Control. Release 286 (February), 10–19. https://doi.org/10.1016/j.jconrel.2018.07.022.
Lichtenstern, C.R., Ngu, R.K., Shalapour, S., Karin, M., 2020. Immunotherapy, Inflammation and Colorectal Cancer. *Cells* 9 (3).
Marques, M., 2004. Dissolution Media Simulating Fasted and Fed States. Dissolut. Technol. 11 (2), 16. https://doi.org/10.14227/DT110204P16.
McConnell, E.L., Basit, A.W., Murdan, S., 2010. Measurements of Rat and Mouse Gastrointestinal PH, Fluid and Lymphoid Tissue, and Implications for in-Vivo Experiments. J. Pharm. Pharmacol. 60 (1), 63–70. https://doi.org/10.1211/jpp.60.1.0008.
McConnell, R.E., Higginbotham, J.N., Shifrin, D.A., Tabb, D.L., Coffey, R.J., Tyska, M.J., 2009. The Enterocyte Microvillus Is a Vesicle-Generating Organelle. J. Cell Biol. 185 (7), 1285–1298. https://doi.org/10.1083/jcb.200902147.
McDonnell, Alison M., Bruce W. S. Robinson, and Andrew J. Currie. 2010. "Tumor Antigen Cross-Presentation and the Dendritic Cell: Where It All Begins?" *Clinical and Developmental Immunology* 2010.
Mescher, M., Tigges, J., Rolfes, K.M., Shen, A.L., Yee, J.S., Vogeley, C., Krutmann, J., Bradfield, C.A., Lang, D., Haarmann-Stemmann, T., 2019. The Toll-like Receptor Agonist Imiquimod Is Metabolized by Aryl Hydrocarbon Receptor-Regulated Cytochrome P450 Enzymes in Human Keratinocytes and Mouse Liver. Arch. Toxicol. 93 (7), 1917–1926. https://doi.org/10.1007/s00204-019-02488-5.
Miller, Mark J., Arsalan S. Hejazi, Sindy H. Wei, Michael D. Cahalan, and Ian Parker. 2004. "T Cell Repertoire Scanning Is Promoted by Dynamic Dendritic Cell Behavior and Random T Cell Motility in the Lymph Node.".
Naxerova, K., Reiter, J.G., Brachtel, E., Lennerz, J.K., van de Wetering, M., Rowan, A., Cai, T., Clevers, H., Swanton, C., Nowak, M.A., Elledge, S.J., Jain, R.K., 2017. Origins of Lymphatic and Distant Metastases in Human Colorectal Cancer. Science 357, 55–60. https://doi.org/10.5061/dryad.vv53d.
Nebaihi, A.I., Hamdah, M., Davies, N.M., Brocks, D.R., 2023. Pharmacokinetics of Cycloheximide in Rats and Evaluation of Its Effect as a Blocker of Intestinal Lymph Formation. Eur. J. Pharm. Biopharm. 193, 89–95. https://doi.org/10.1016/j.ejpb.2023.10.016.
Patente, Thiago A., Mariana P. Pinho, Aline A. Oliveira, Gabriela C. M. Evangelista, Patrícia C. Bergami-Santos, and José A. M. Barbuto. 2019. "Human Dendritic Cells: Their Heterogeneity and Clinical Application Potential in Cancer Immunotherapy." *Frontiers in Immunology* 10(JAN):1–18. doi: 10.3389/fimmu.2018.03176.
Porter, C.J.H., Trevaskis, N.L., Charman, W.N., 2007. Lipids and lipid-based formulations: optimizing the oral delivery of lipophilic drugs. Nat. Rev. Drug Discov. 6 (3), 231–248.
Qin, C., Chu, Y.J., Feng, W., Fromont, C., He, S., Ali, J., Lee, J.B., Zgair, A., Berton, M., Bettonte, S., Liu, R., Yang, L., Monmaturapoj, T., Medrano-Padial, C., Ugalde, A.A.R., Vetrugno, D., Ee, S.Y., Sheriston, C., Yuntao, Wu., Stocks, M.J., Fischer, P.M., Gershkovich, P., 2020. Targeted Delivery of Lopinavir to HIV Reservoirs in the Mesenteric Lymphatic System by Lipophilic Ester Prodrug Approach. *J. Control. Release* (october). https://doi.org/10.1016/j.jconrel.2020.10.036.
Quach, T., Luojuan, Hu., Han, S., Lim, S.F., Senyschyn, D., Yadav, P., Trevaksis, N.L., Simpson, J.S., Porter, C.J.H., 2022. Triglyceride-Mimetic Prodrugs of Buprenorphine Enhance Oral Bioavailability via Promotion of Lymphatic Transport. Front. Pharmacol. 13. https://doi.org/10.3389/fphar.2022.879660.
Redden, Peter, R., Rhea L. Melanson, Jo-Anne E. Douglas, and Arthur J. Dick. 1999. *Acyloxymethyl Acidic Drug Derivatives: In Vitro Hydrolytic Reactivity*. Vol. 180.
Reiter, M.J., Testerman, T.L., Miller, R.L., Weeks, C.E., Tomai, M.A., 1994. Cytokine Induction in Mice by the Immunomodulator Imiquimod. J. Leukoc. Biol. 55 (2), 234–240. https://doi.org/10.1002/jlb.55.2.234.
Sabado, R.L., Balan, S., Bhardwaj, N., 2017. Dendritic Cell-Based Immunotherapy. Cell Res. 27 (1), 74–95. https://doi.org/10.1038/cr.2016.157.
Sasaki, T., Shigeta, K., Matsui, S., Seishima, R., Okabayashi, K., Kitagawa, Y., 2023. Mesenteric Location of Lymph Node Metastasis for Colorectal Cancer. ANZ J. Surg. 93 (5), 1257–1261. https://doi.org/10.1111/ans.18221.
Savage, P., Horton, V., Moore, J., Owens, M., Witt, P., Gore, M.E., 1996. A Phase I Clinical Trial of Imiquimod, an Oral Interferon Inducer, Administered Daily. Br. J. Cancer 74 (9), 1482–1486. https://doi.org/10.1038/bjc.1996.569.
Schumacher-Klinger, A., Fanous, J., Merzbach, S., Weinmüller, M., Reichart, F., Räder, A. F.B., Gitlin-Domagalska, A., Gilon, C., Kessler, H., Hoffman, A., 2018. Enhancing Oral Bioavailability of Cyclic RGD Hexa-Peptides by the Lipophilic Prodrug Charge Masking Approach: Redirection of Peptide Intestinal Permeability from a Paracellular to Transcellular Pathway. Mol. Pharm. 15 (8), 3468–3477. https://doi.org/10.1021/acs.molpharmaceut.8b00466.
Shayeganpour, A., Hamdy, D.A., Brocks, D.R., 2008. Pharmacokinetics of Desethylamiodarone in the Rat after Its Administration as the Preformed Metabolite, and after Administration of Amiodarone. Biopharm. Drug Dispos. 29 (3), 159–166. https://doi.org/10.1002/bdd.599.
Shu, P., Ouyang, G., Wang, F., Zhou, J., Shen, Y., Li, Z., Wang, X., 2020. The role of radiotherapy in the treatment of retroperitoneal lymph node metastases from colorectal cancer. Cancer Manag. Res. 12, 8913–8921. https://doi.org/10.2147/CMAR.S249248.
Shukla, N.M., Malladi, S.S., Mutz, C.A., Balakrishna, R., David, S.A., 2010. Structure-Activity Relationships in Human Toll-like Receptor 7-Active Imidazoquinoline Analogues. J. Med. Chem. 53 (11), 4450–4465. https://doi.org/10.1021/jm100358c.
Sidky, Y.A., Borden, E.C., Weeks, C.E., Reiter, M.J., Hatcher, J.F., Bryan, G.T., 1992. Inhibition of Murine Tumor Growth by an Interferon-Inducing Imidazoquinolinamine. Cancer Res. 52 (13), 3528–3533.
Simplício, A.L., Clancy, J.M., Gilmer, J.F., 2008. Prodrugs for Amines. Molecules 13 (3), 519–547. https://doi.org/10.3390/molecules13030519.
Smith, M., García-Martínez, E., Pitter, M.R., Fucikova, J., Spisek, R., Zitvogel, L., Kroemer, G., Galluzzi, L., 2018. Trial watch: toll-like receptor agonists in cancer immunotherapy. OncoImmunology 7 (12), 1–15. https://doi.org/10.1080/2162402X.2018.1526250.
Soria, I., Myhre, P., Horton, V., Ellefson, P., McCarville, S., Schmitt, K., Owens, M., 2000. Effect of Food on the Pharmacokinetics and Bioavailability of Oral Imiquimod Relative to a Subcutaneous Dose. Int. Journal of Clinical Pharmacology and Therapeutics 38 (10), 476–481. https://doi.org/10.5414/CPP38476.
Stacker, S.A., Williams, S.P., Karnezis, T., Shayan, R., Fox, S.B., Achen, M.G., 2014. Lymphangiogenesis and Lymphatic Vessel Remodelling in Cancer. Nat. Rev. Cancer 14 (3), 159–172.
Tilney, N.L., 1971. Patterns of Lymphatic Drainage in the Adult Laboratory Rat. J. Anat. 109 (Pt 3), 369–383.
Jianyong Wang. 2010. "PHARMACOLOGY/TOXICOLOGY NDA REVIEW AND EVALUATION APPLICATION NUMBER: 201153Orig1s000." *Department of Health and Human Services Public Health Service FOOD AND DRUG ADMINISTRATION CERTER FOR DRUG EVALUATION AND RESEARCH*.
Neena Washington, Clive Washington, and Clive Wilson. 2000. "Chapter Seven: Drug Delivery to the Large Intestine and Rectum." Pp. 114–79 in *Physiological Pharmaceutics*. London.
Wculek, S.K., Cueto, F.J., Mujal, A.M., Melero, I., Krummel, M.F., Sancho, D., 2020. Dendritic Cells in Cancer Immunology and Immunotherapy. Nat. Rev. Immunol. 20 (1), 7–24. https://doi.org/10.1038/s41577-019-0210-z.
Wu, Y.-H., Tom, M.S., Miller, A.T., De Gregorio, E., Doro, F., David, A.G., Skibinski, M.L., Mbow, S.B., Herman, A.E., Cortez, A., Li, Y., Nayak, B.P., Tritto, E., Filippi, C.M., Otten, G.R., Brito, L.A., Monaci, E., Li, C., Aprea, S., Valentini, S., Calabró, S., Laera, D., Brunelli, B., Caproni, E., Malyala, P., Panchal, R.G., Warren, T.K.,

Bavari, S., Derek, T.O., 2014. Rational Design of Small Molecules as Vaccine Adjuvants. ADJUVANTS 6 (263). https://doi.org/10.1126/scitranslmed.3009980.

Xiao, C., Stahel, P., Lewis, G.F., 2019. Regulation of Chylomicron Secretion: Focus on Post-Assembly Mechanisms. Cmgh 7 (3), 487–501. https://doi.org/10.1016/j.jcmgh.2018.10.015.

Yáñez, J.A., Wang, S.W.J., Knemeyer, I.W., Wirth, M.A., Alton, K.B., 2011. Intestinal Lymphatic Transport for Drug Delivery. Adv. Drug Deliv. Rev. 63 (10–11), 923–942. https://doi.org/10.1016/j.addr.2011.05.019.

Yeo, S.G., Kim, D.Y., Kim, T.H., Jung, K.H., Hong, Y.S., Kim, S.Y., Park, J.W., Choi, H.S., Jae Hwan, Oh., 2010. Curative Chemoradiotherapy for Isolated Retroperitoneal Lymph Node Recurrence of Colorectal Cancer. Radiother. Oncol. 97 (2), 307–311. https://doi.org/10.1016/j.radonc.2010.05.021.

Yin, W., Xuan, D., Wang, H., Zhou, M., Deng, B., Fang Ma, Y.L., Zhang, J., 2022. Biodegradable Imiquimod-Loaded Mesoporous Organosilica as a Nanocarrier and Adjuvant for Enhanced and Prolonged Immunity against Foot-and-Mouth Disease Virus in Mice. ACS Appl. Bio Mater. 5 (6), 3095–3106. https://doi.org/10.1021/acsabm.2c00382.

Yin, W., Deng, B., Zeyu, Xu., Wang, H., Ma, F., Mingxu Zhou, Y.L., Zhang, J., 2023. Formulation and Evaluation of Lipidized Imiquimod as an Effective Adjuvant. ACS Infect. Dis. 9 (2), 378–387. https://doi.org/10.1021/acsinfecdis.2c00583.

Zgair, Atheer, Jong Bong Lee, Jonathan C. M. Wong, Dhiaa A. Taha, Jehan Aram, Daisy Di Virgilio, Joshua W. McArthur, Yu Kit Cheng, Ivo M. Hennig, David A. Barrett, Peter M. Fischer, Cris S. Constantinescu, and Pavel Gershkovich. 2017. "Oral Administration of Cannabis with Lipids Leads to High Levels of Cannabinoids in the Intestinal Lymphatic System and Prominent Immunomodulation." *Scientific Reports* 7 (1). doi: 10.1038/s41598-017-15026-z.

Zgair, A., Wong, J.C.M., Lee, J.B., Mistry, J., Sivak, O., Wasan, K.M., Hennig, I.M., Barrett, D.A., Constantinescu, C.S., Fischer, P.M., Gershkovich, P., 2016. Dietary fats and pharmaceutical lipid excipients increase systemic exposure to orally administered cannabis and cannabis-based medicines. Am. J. Transl. Res. 8 (8), 3448–3459.

Zhu, Shaoming, Tian Zhang, Lei Zheng, Hongtao Liu, Wenru Song, Delong Liu, Zihai Li, and Chong xian Pan. 2021. "Combination Strategies to Maximize the Benefits of Cancer Immunotherapy." *Journal of Hematology and Oncology* 14(1).